# The Kuiper Belt and Other Debris Disks

David Jewitt, Amaya Moro-Martín and Pedro Lacerda

**Abstract** We discuss the current knowledge of the Solar system, focusing on bodies in the outer regions, on the information they provide concerning Solar system formation, and on the possible relationships that may exist between our system and the debris disks of other stars. Beyond the domains of the Terrestrial and giant planets, the comets in the Kuiper belt and the Oort cloud preserve some of our most pristine materials. The Kuiper belt, in particular, is a collisional dust source and a scientific bridge to the dusty "debris disks" observed around many nearby main-sequence stars. Study of the Solar system provides a level of detail that we cannot discern in the distant disks while observations of the disks may help to set the Solar system in proper context.

## 1 Introduction

Planetary astronomy is unusual among the astronomical sciences in that the objects of its attention are inexorably transformed by intensive study into the targets of other sciences. For example, the Moon and Mars were studied telescopically by astronomers for nearly four centuries but, in the last few decades, these worlds have been transformed into the playgrounds of geologists, geophysicists, meteorologists, biologists and others. Telescopic studies continue to be of value, but we now learn most about the Moon and Mars from in-situ investigations. This transformation from science at-a-distance to science up-close is a forward step and a tremendous luxury not afforded to the rest of astronomy. Those who study other stars or the galaxies beyond our own will always be forced by distance to do so telescopically.

David Jewitt and Pedro Lacerda
Institute for Astronomy, University of Hawaii, e-mail: jewitt@ifa.hawaii.edu

Amaya Moro-Martín
Dept. Astronomy, Princeton University e-mail: amaya@astro.princeton.edu

However, the impression that the Solar system is now *only* geology or meteorology or some other science beyond the realm of astronomy is completely incorrect when applied to the outer regions. The Outer Solar system (OSS) remains firmly entrenched within the domain of astronomy, its contents accessible only to telescopes. Indeed, major components of the OSS, notably the Kuiper belt, were discovered (telescopically) less than two decades ago and will continue to be best studied via. astronomical techniques for the foreseeable future. It is reasonable to expect that the next generation of telescopes in space and on the ground will play a major role in improving our understanding of the Solar system, its origin and its similarity to related systems around other stars.

In this chapter, we present an up-to-date overview of the layout of the Solar system and direct attention to the outer regions where our understanding is the least secure but the potential for scientific advance is the greatest. The architecture of the Kuiper belt is discussed as an example of a source-body system that probably lies behind many of the debris disks of other stars. Next, the debris disks are discussed based on the latest observations from the ground and from Spitzer, and on new models of dust transport. Throughout, we use text within grey boxes to highlight areas where the Next Generation telescopes are expected to have major impact.

## 2 The Architecture of the Solar System

It is useful to divide the Solar system into three distinct domains, those of the Terrestrial planets, the giant planets, and the comets. Objects within these domains are distinguished by their compositions, by their modes of formation and by the depth and quality of knowledge we possess on each.

### *2.1 Terrestrial Planets*

The Terrestrial planets (Mercury, Venus, Earth and Moon, Mars and most main-belt asteroids) are found inside 3 AU. They have refractory compositions dominated by iron ($\sim$ 35% by mass), oxygen ($\sim$ 30%), silicon and magnesium ($\sim$15% each) and were formed by binary accretion in the protoplanetary disk. About 95% of the Terrestrial planet mass is contained within Venus and Earth ($\sim$1 $M_\oplus = 6\times10^{24}$ kg, each). The rest is found in the small planets Mercury and Mars, with trace amounts ($\sim 3\times10^{-4}$ $M_\oplus$) in the main-belt asteroids located between Mars and Jupiter. The largest asteroid is Ceres ($\sim$ 900 km diameter). The Terrestrial planets grew by binary accretion between solid bodies in the protoplanetary disk of the Sun. While not all details of this process are understood, it is clear that sticking and coagulation of dust grains, perhaps aided at first by hydrodynamic forces exerted from the gaseous component of the disk, produced larger and larger bodies up to the ones we see now in the Solar system. The gaseous component, judged mainly by observations of other

stars, dissipated on timescales from a few to $\sim$10 Myr. Measurements of inclusions within primitive meteorites show that macroscopic bodies existed within a few Myr of the origin. The overall timescale for growth was determined, ultimately, by the sweeping up of residual mass from the disk, a process thought to have taken perhaps 40 Myr in the case of the Earth. No substantial body is found in the asteroid belt although it is likely that sufficient mass existed there to form an object of planetary class. This is thought to be because growth in this region was interrupted by strong perturbations, caused by the emergence of nearby, massive Jupiter (at $\sim$5 AU).

## *2.2 Giant Planets*

Orbits of the giant planets (Jupiter, Saturn, Uranus and Neptune) span the range 5 AU to 30 AU. The giants are in fact of two compositionally distinct kinds.

### 2.2.1 Gas Giants

Jupiter (310 $M_\oplus$) and Saturn (95 $M_\oplus$) are so-called because, mass-wise, they are dominated by hydrogen and helium. Throughout the bulk of each planet these gases are compressed, however, into a degenerate (metallic) liquid that supports convection and sustains a magnetic field through dynamo action. The compositional similarity to the Sun suggests to some investigators that the gas giants might form by simple hydrodynamic collapse of the protoplanetary gas nebula (Boss 2001). In hydrodynamic collapse the essential timescale is given by the free-fall time, and this could be astonishingy short (e.g. 1000 yrs). Details of this instability, especially related to the necessarily rapid cooling of the collapsing planet, remain under discussion (Boley et al. 2007, Boss 2007). In fact, measurements of the moment of inertia, coupled with determinations of the equation of state of hydrogen-helium mixtures at relevant pressures and temperatures, show that Saturn (certainly) and Jupiter (probably) have distinct cores containing 5 $M_\oplus$ to 15 $M_\oplus$ of heavy elements (the case of Jupiter is less compelling than Saturn because of its greater mass and central hydrostatic pressure, leading to larger uncertainties concerning the self-compressibility of the gas). The presence of a dense core is the basis for the model of formation through " nucleated instability", in which the core grows by binary accretion in the manner of the Terrestrial planets, until the gravitational escape speed from the core becomes comparable to the thermal speed of molecules in the gas nebula. Then, the core traps gas directly from the nebula, leading to the large masses and gas-rich compositions observed in Jupiter and Saturn.

Historically, the main sticking point for nucleated instability models has been that the cores must grow to critical size *before* the surrounding gas nebula dissipates (i.e. 5 $M_\oplus$ to 15 $M_\oplus$ cores must grow in much less than 10 Myr). The increase in the disk surface density due to the freezing of water as ice outside the snow-line is one factor helping to decrease core growth times. Another may be the radial jumping

motion of the growing cores, driven by angular momentum and energy exchange with planetesimals (Rice and Armitage 2003). In recent times, a consensus appears to have emerged that Jupiter's core, at least, could have grown by binary accretion from a disk with $\Sigma \sim 50$ to 100 kg m$^{-2}$ on timescales $\sim$1 Myr (Rice and Armitage 2003). The collapse of nebular gas onto the core after this would have been nearly instantaneous.

Recent data show that the heavier elements (at least in Jupiter, the better studied of the gas giants) are enriched relative to hydrogen in the Sun by factors of $\sim$2 to 4 (Owen et al. 1999), so that wholesale nebular collapse cannot be the whole story (and may not even be part of it). The enrichment applies not only to species that are condensible at the $\sim$100 K temperatures appropriate to Jupiter's orbit, but to the noble gases Ar, Kr and Xe, which can only be trapped in ice at much lower temperatures, $<$30 K (e.g. Bar-Nun et al. 1988) . Therefore, Owen et al. suggest that the gas giants incorporate substantial mass from a hitherto unsuspected population of ultracold bodies, presumably originating in the outer Solar system. In a variant of this model, cold grains from the outer Solar system trap volatile gases but drift inwards under the action of gas drag, eventually reaching the inner nebula when they evaporate in the heat of the Sun and enrich the gas (Guillot and Huesco 2006).

### 2.2.2 Ice Giants

Uranus (15 $M_\oplus$) and Neptune (17 $M_\oplus$), in addition to being an order of magnitude less massive than the gas giants are compositionally distinct. These planets contain a few $M_\oplus$ of H and He, and a much larger fraction of the "ices" $H_2O$, $CH_4$ and $NH_3$. For this reason they are known as "ice giants", but the name is misleading because they are certainly not solid bodies but are merely composed of molecules which, if they were much colder, would be simple ices. In terms of their mode of formation, the difference between the ice giants and the gas giants may be largely one of timescale. It is widely thought that the ice giants correspond to the heavy cores of Jupiter and Saturn, but with only vestigial hydrogen/helium envelopes accreted from the rapidly dissipating gaseous component of the protoplanetary disk.

While qualitatively appealing, forming Uranus and (especially) Neptune on the 10 Myr timescale associated with the loss of the gas disk has been a major challenge to those who model planetary growth. The problem is evident from a simple consideration of the collision rate between particles in a disk or surface density $\Sigma(R)$ kg m$^{-2}$, where $R$ is the heliocentric distance. The probability of a collision in each orbit varies in proportion to $\Sigma(R)$, while the orbital period varies as $R^{3/2}$. Together, this gives a collision timescale varying as $R^{3/2}/\Sigma(R)$ which, with $\Sigma(R) \propto R^{-3/2}$ gives $t_c \propto R^3$. A giant planet core that takes 1 Myr to form at 5 AU would take $6^3 \sim$200 Myr to form at 30 AU, and this considerably exceeds the gas disk lifetime. Suggested solutions to the long growth times for the outer planets include augmentation of the disk density, $\Sigma(R)$, perhaps through the action of aerodynamic drag, and formation of the ice giants at smaller distances (and therefore higher $\Sigma$) than those at which they reside. The latter possibility ties into the general notion that the orbits

of the outermost three planets have expanded in response to the action or torques between the planets and the disk. Still another idea is that Uranus and Neptune are gas giants whose hydrogen and helium envelopes were ablated by ionizing radiation from the Sun or a nearby, hot star (Boss et al. 2002).

## *2.3 Comets*

Comets are icy bodies which sublimate in the heat of the Sun, producing observationally diagnostic unbound atmospheres or "comae". For most known comets, the sublimation is sufficiently strong that mass loss cannot be sustained for much longer than $\sim 10^4$ yr, a tiny fraction of the age of the Solar system. For this reason, the comets must be continually resupplied to the planetary region from one or more low temperature reservoirs, if their numbers are to remain in steady state. In the last half century, at least three distinct source regions have been identified.

### 2.3.1 Oort Cloud Comets

The orbits of long period comets are highly elliptical, isotropically distributed and typically large (Figure 1), suggesting a gravitationally bound, spheroidal source region of order 100,000 AU in extent (Oort 1950). Comets in the cloud are scattered randomly into the planetary region by the action of passing stars and also perturbed by the asymmetric gravitational potential of the galactic disk (e.g. Higuchi et al. 2007). Unfortunately, the cloud is so large that its residents cannot be directly counted. The population must instead be inferred from the rate of arrival of comets from the cloud and estimates of the external torques. A recent work gives the number larger than $\sim$1 km in radius as $5\times10^{11}$, with a combined mass in the range $2M_\oplus$ to $40M_\oplus$ (Francis 2005).

Oort cloud comets are thought to have originated in the Sun's protoplanetary disk in the vicinity of the giant planets and were scattered out by interactions with the growing, migrating planetary embryos. Although most were lost, a fraction of the ejected comets, perhaps from 1% to 10%, was subsequently deflected by external perturbations that lifted the perihelia out of the planetary region, effectively decoupling these comets from the rest of the system (Hahn and Malhotra 1999). Over $\sim$1 Gyr, the orbits of trapped comets were randomized, converting their distribution from a flattened one reflecting their disk source to a spherical one, compatible with the random directions of arrival of long period comets. In this model, which is qualitatively unchanged from that proposed by Oort (1950), the scale and population of the Oort cloud are set by the external perturbations from nearby stars and the galactic disk. If the Sun formed in a cluster, then the average perturbations from cluster members would have been bigger than now and a substantial population of more tightly bound, so-called "inner Oort cloud" comets could have been trapped. It is possible that the Halley family comets, whose orbits are predominantly but not

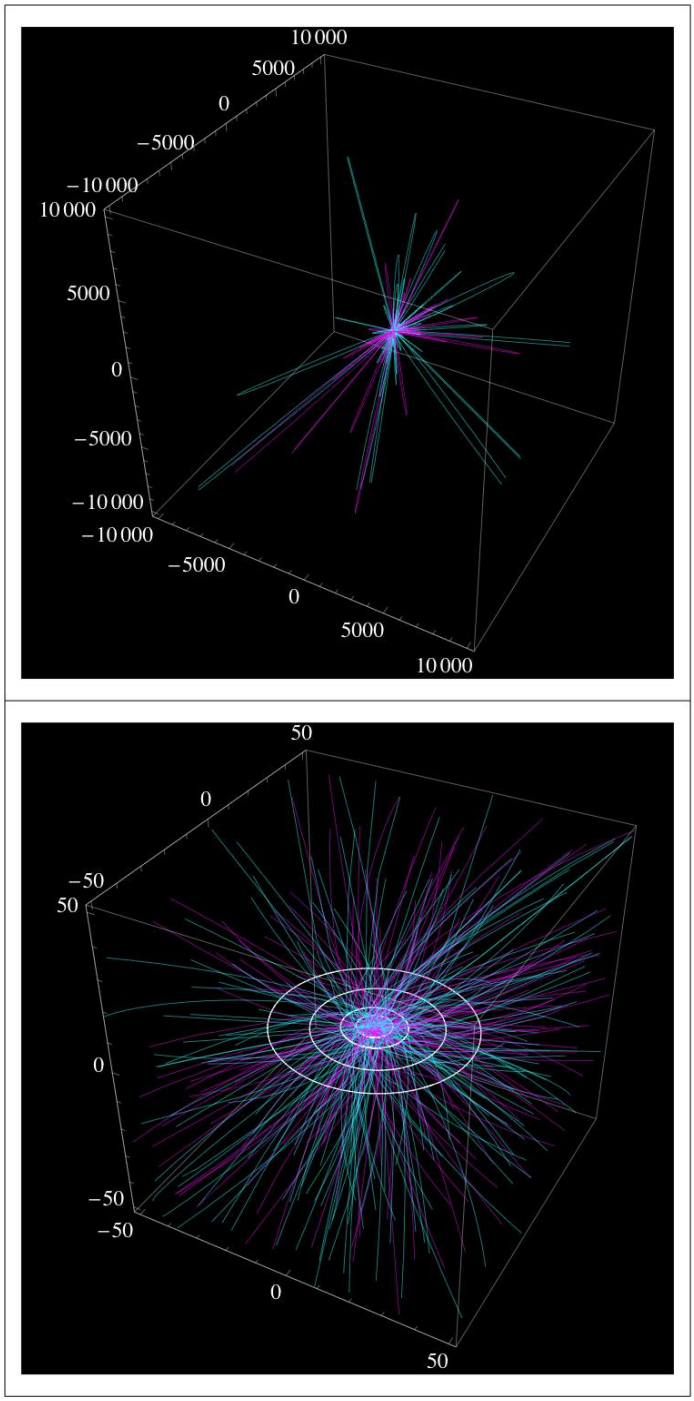


**Fig. 1** Orbits of the nearly 200 long period comets (orbital period, $P > 200$ yrs) listed in the JPL small-body database. The highly eccentric orbits of many LPCs appear as nearly radial lines on the top (wide angle) view, showing a cube 20,000 AU on a side. The bottom panel shows a narrow angle view of a 100 AU cube. Prograde orbits are shown in cyan while retrograde orbits are in magenta. Numbers along the axes are distances in AU from the Sun at (0,0,0). The orbits of the giant planets are shown in white.

exclusively prograde (Figure 2) are delivered from the inner Oort cloud (Levison et al. 2001).

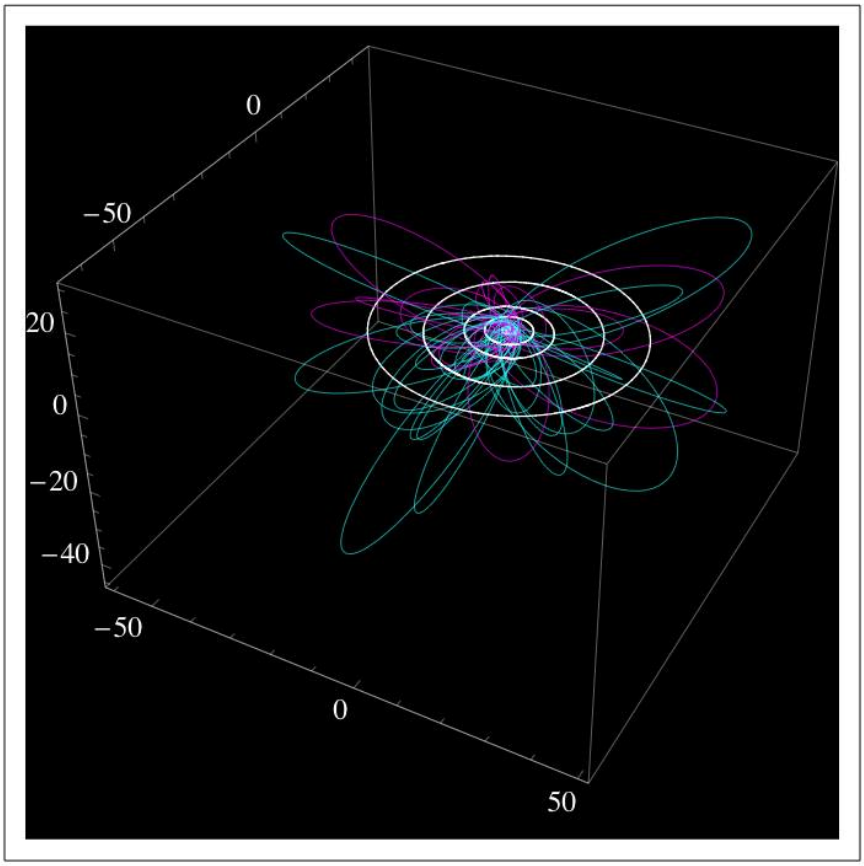


**Fig. 2** Halley family comets. Their non-isotropic inclination distribution, with more prograde (cyan) orbits than retrograde (magenta), points to an origin in the inner Oort cloud, where stellar and galactic perturbations have been too small to randomize the orbits. Following the classical definition, we plot the 44 comets in the JPL small-body database having Tisserand parameters with respect to Jupiter $\leq 2$ and orbital periods $20 < P(\text{yrs}) < 200$. The orbits of the giant planets are shown in white.

Some 90% to 99% of the comets formed in our system eluded capture and now roam the interstellar medium. If this fraction applies to all stars, then $\sim 10^{23}$ to $\sim 10^{24}$ "interstellar comets" exist in our galaxy, containing several $\times 10^5$ $M_\odot$ of metals. Interstellar comets ejected from other stars might be detected with all-sky surveys in the Pan STARRS or Large Synoptic Survey Telescope (LSST) class (Je-

witt 2003). Such objects would be recognized by their strongly hyperbolic orbits relative to the Sun, quite different from any object yet observed.

### 2.3.2 Kuiper Belt Comets

The orbits of the Jupiter family comets (JFCs) have modest inclinations, with no retrograde examples, and most have eccentricities much less than unity (Figure 3). They are dynamically distinct from the long period Oort comets, and they interact strongly with Jupiter. For many years it was thought that the JFCs were captured from the long period population by Jupiter but increasingly numerical detailed work in the 1980's showed that this was not possible (Fernández 1980, Duncan et al. 1988). The source appears to be the Kuiper belt, although this is not an iron-clad conclusion and the particular region or regions in the Kuiper belt from which the JFCs originate has yet to be identified.

About 200 JFCs are numbered (meaning that their orbits are very well determined) and a further 200 are known. Their survival is limited by a combination of volatile depletion, ejection from the Solar system, or impact into a planet or the Sun. Dynamical interactions alone give a median lifetime near 0.5 Myr (Levison and Duncan 1994), which matches the volatile depletion lifetime for bodies smaller than $r \sim 40$ km. The implication is that JFCs smaller than this size will become dormant before they are dynamically removed, ending up as bodies that are asteroidal in appearance but cometary in orbit. Some of these dead comets are suspected to exist among the near-Earth "asteroid" population; indirect evidence for a fraction $\sim 10\%$ comes from albedo measurements (Fernández et al. 2001) and dynamical models (Bottke et al. 2002).

### 2.3.3 Main Belt Comets

At the time of writing (February 2008) three objects are known to have the dynamical characteristics of asteroids but the physical appearances of comets. They show comae and particle tails indicative of on-going mass loss (Hsieh and Jewitt, 2006; Figures 4 and 5). These are the Main-Belt comets (MBCs), most directly interpreted as ice-rich asteroids.

In the modern Solar system, the MBCs are dynamically isolated from the Oort cloud and Kuiper belt reservoirs (i.e. they cannot be captured from these other regions given the present-day layout of the Solar system, c.f. Levison et al. 2006). The MBCs should thus be regarded as a third and independent comet reservoir. Two possibilities for their origin seem plausible. The MBCs could have accreted ice if they grew in place but outside the snow-line. Alternatively, the MBCs might have been captured from elsewhere if the layout of the Solar system were very different in the past, providing a dynamical paths from the Kuiper belt that do not now exist. Insufficient evidence exists at present to decide between these possibilities.

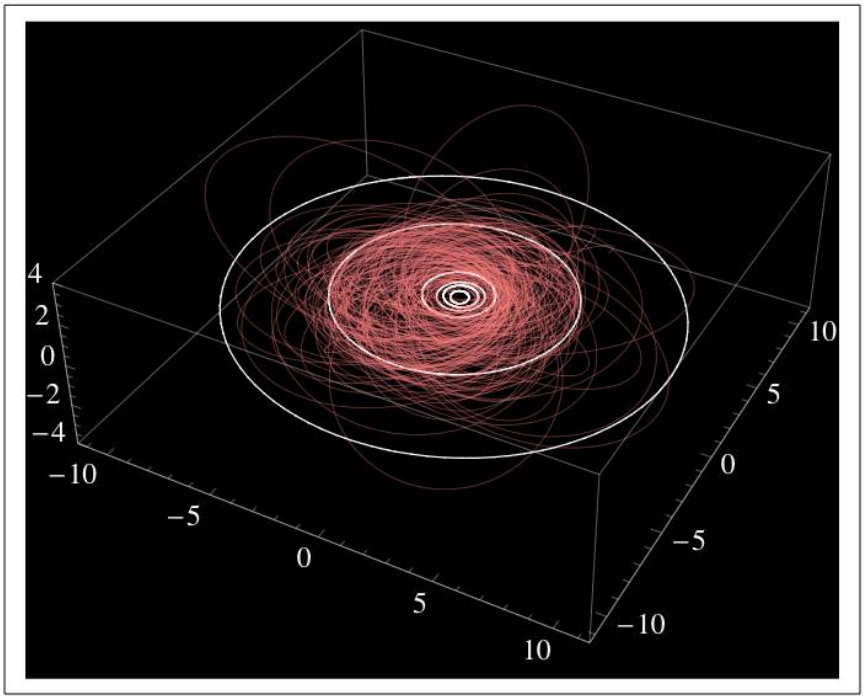


**Fig. 3** Perspective view of the Jupiter family comets (salmon) together with the orbits of the planets out to Saturn. The Sun is at $(x,y,z) = (0,0,0)$ and the distances are in AU. Plotted are 166 JFCs, selected from the JPL small-body database based on their Tisserand parameter with respect to Jupiter ($2 < T_J < 3$; see, e.g., Levison and Duncan 1994) and with orbital periods $P < 20$ yr.

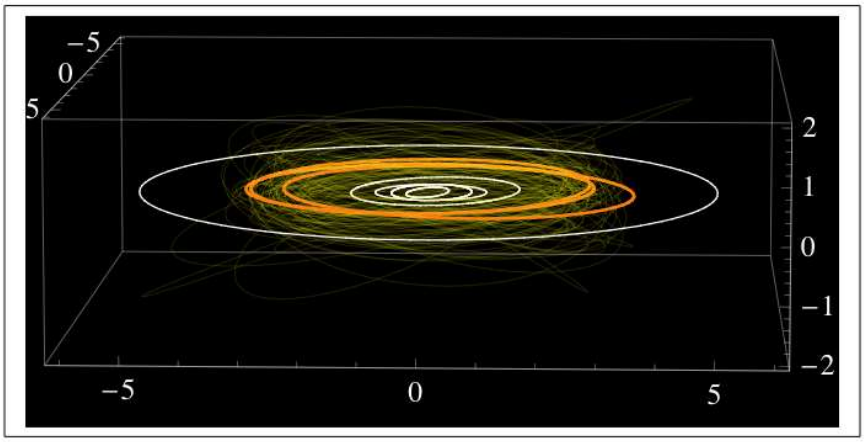


**Fig. 4** Perspective view of the main-belt comets (orange) together with the orbits of 100 asteroids (thin, yellow lines) and planets out to Jupiter.

These bodies escaped detection until now because their mass loss rates ($\ll 1$ kg $s^{-1}$) are two to three orders of magnitude smaller than from typical comets. The mass loss is believed to be driven by the sublimation of water ice exposed in small surface regions, with effective sublimating areas of $\sim$1000 $m^{-2}$ and less. Although sublimation at 3 AU is weak, the MBCs are small and mass loss at the observed rates cannot be sustained for the age of the Solar system. Instead, a trigger for the activity (perhaps impact excavation of otherwise buried ices) is needed. This raises the possibility that the detected MBCs are a tiny fraction of the total number that will be found by dedicated surveys like *Pan STARRS* and *LSST*. Even more interesting is the possibility that many or even most outer belt asteroids are in fact ice-rich bodies which display only transient activity. Evidence from the petrology and mineralogy of meteorites (e.g. the CI and CM chondrites that are thought to originate in the outer belt) shows the past presence of liquid water in the meteorite parent bodies. The MBCs show that some of this water survived to the present day.

**Next generation** facilities will offer opportunities to study the physical properties of the satellite systems of the giant planets. The regular satellites occupy prograde orbits of small inclination and eccentricity, resulting from their formation in the accretion disks through which the planets grew. As such, the individual regular satellite systems offer information about the sub-nebulae that must have existed around the growing planets. These sub-nebulae had their own density and temperature structures very different from the local disk of the Sun. Studies of reflected and thermal radiation with *JWST* and *ALMA* will be able to determine compositional differences in even the fainter regular satellites of the ice giants, and may provide constraints on Io-like and Enceladus-like endogenous activity.

The study of comets will be greatly advanced by *JWST* spectroscopy of the nuclei of comets (in order to minimize the effects of scattering from the dust coma, these small objects must be observed when far from the Sun and therefore faint). Simultaneous measurements of reflected and thermal radiation will provide albedo measurements which, with high signal-to-noise ratio spectra, will help determine the nature and evolution of the refractory surface mantles of these bodies.

## 3 Kuiper Belt

More than 1200 Kuiper belt objects (KBOs) have been discovered since the first example, 1992 QB1, was identified in 1992. The known objects have typical diameters of 100 km and larger. The total number of such objects, scaled from published surveys, is of order 70,000, showing that there is considerable remaining discovery

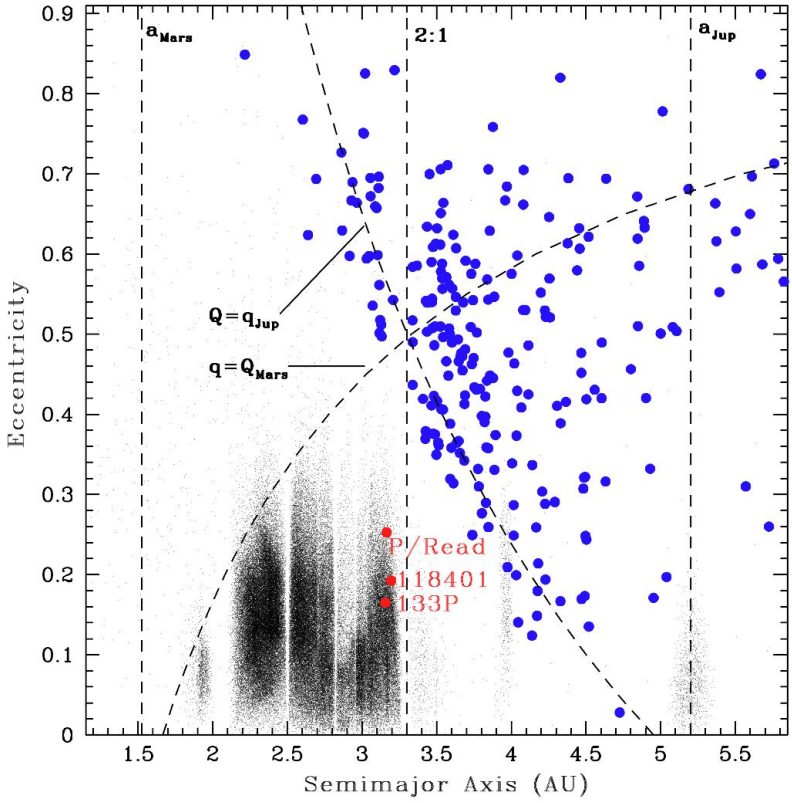


**Fig. 5** Orbital semimajor axis vs. eccentricity for objects classified as asteroids (black) and comets (blue), together with the three known main-belt comets 133P/Elst-Pizarro, P/2005 U1 (Read), and 118401 (1999 $RE_{70}$) (plotted in red). Vertical dashed lines mark the semimajor axes of Mars and Jupiter and the 2:1 mean-motion resonance with Jupiter (commonly considered the outer boundary of the classical main belt), as labeled. Curved dashed lines show the loci of orbits with perihelia equal to Mars's aphelion ($q = Q_{Mars}$) and orbits with aphelia equal to Jupiter's perihelion ($Q = q_{Jup}$). Objects plotted above the $q > Q_{Mars}$ line are Mars-crossers. Objects plotted to the right of the $Q < q_{Jup}$ line are Jupiter-crossers. From Hsieh and Jewitt (2006).

space to be filled by future surveys. The number of objects larger than 1 km may exceed $10^8$.

The KBO orbits occupy a thick disk or sheet outside Neptune's orbit (Figure 6). A major observational result is the finding that the KBOs can be divided on the basis of their orbital elements into several, distinct groups (Jewitt et al. 1998). This is best seen in $a$ (semimajor axis) vs. $e$ (orbital eccentricity) space, shown here in Figure 7. The major Kuiper belt dynamical groups in the figure are

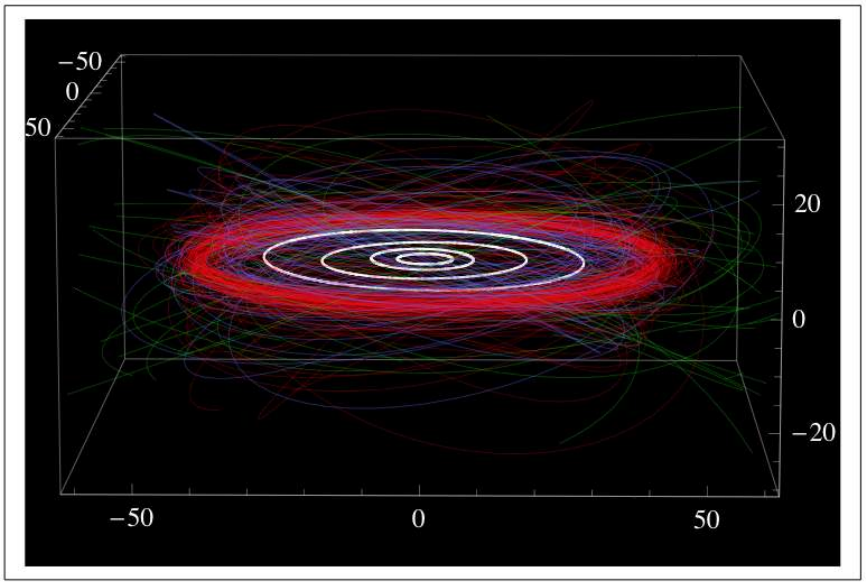


**Fig. 6** Perspective view of the Kuiper belt. The Sun is at $(x,y,z) = (0,0,0)$ and the axes are marked in AU. White ellipses show the orbits of the four giant planets. Red orbits mark the classical KBOs. Their ring-like distribution is obvious. Blue orbits show resonant KBOs, while green shows the Scattered objects. For clarity, only one fifth of the total number of objects in each dynamical type is plotted.

- Classical Kuiper belt objects (red circles). These orbit between about $a$ = 42 AU and the 2:1 mean-motion resonance with Neptune at $a$ = 47 AU. Typical orbital eccentricities of the Classicals are $e \sim 0$ to 0.2 while the inclination distribution appears to be bimodal with components near $i = 2^\circ$ (so-called "Cold-Classicals) and $i = 20^\circ$ (the "Hot Classicals", Brown and Trujillo 2001, Elliot et al. 2005). Numerical integrations show that the orbits of the Classical objects are stable on timescales comparable to the age of the Solar system largely because their perihelia are always so far from Neptune's orbit that no strong scattering occurs.

- Resonant Kuiper belt objects (blue circles). A number of mean-motion resonances (MMRs) with Neptune are populated by KBOs, especially the 3:2 MMR at 39.3 AU and the 2:1 MMR at 47.6 AU (see Figure 7). The 3:2 MMR objects are known as Plutinos, to recognize 134340 Pluto as the first known member of this population. The 2:1 MMR objects are sometimes called "twotinos" while those in 1:1 MMR are Neptune's Trojans (Sheppard and Trujillo 2006). The resonant objects are dynamically stable by virtue of phase protections conferred by the resonances. For example, KBOs in 3:2 MMR can, like Pluto itself, have perihelia inside Neptune's orbit, but their orbits librate under perturbations from that planet in such a way that the distance of closest approach to Neptune is always

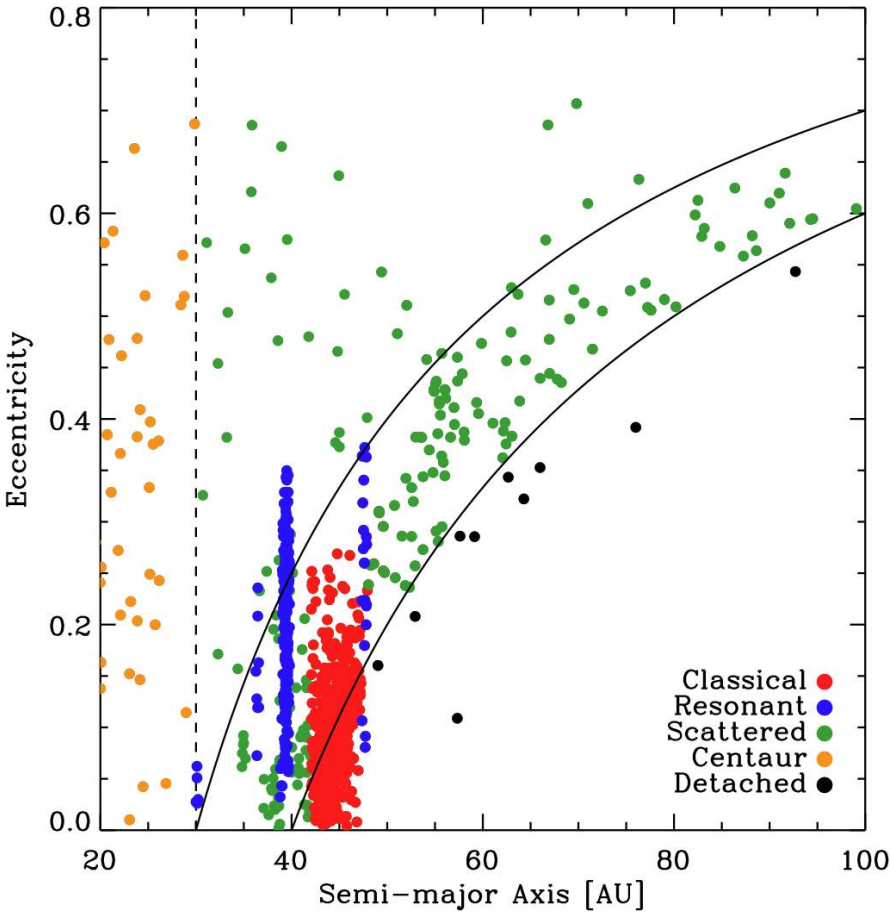


**Fig. 7** Orbital semimajor axis vs. eccentricity for KBOs known as of 2008 January 30. The objects are color-coded according to their dynamical type, as labeled in the Figure and discussed in the text. A vertical dashed line at $a$ = 30 AU marks the orbit of Neptune, the nominal inner-boundary of the Kuiper belt. Upper and lower solid arcs show the loci of orbits having perihelion distances $q = a(1-e)$ equal to 30 AU and 40 AU, respectively.

large. In fact, all objects above the upper solid arc in Figure 7 have perihelia interior to Neptune's orbit.

The process by which KBOs became trapped in MMRs is thought to be planetary migration (Fernández and Ip 1984). Migration occurs as a result of angular momentum transfer during gravitational interactions between the planets and material in the disk. At late stages in the evolution of the disk (i.e. later than $\sim$10 Myr, after the gaseous component of the disk has dissipated) the interactions are between the planets and individual KBOs or other planetesimals. In a one-planet system, the sling-shot ejection of KBOs to the interstellar medium would result

in net shrinkage of the planetary orbit. In the real Solar system, however, KBOs can be scattered inwards from planet to planet, carrying energy and angular momentum with them as they go. Massive Jupiter then acts as the source of angular momentum and energy, ejecting KBOs from the system. In the process, its orbit shrinks, while those of the other giant planets expand. The timescale is the same as the timescale for planetary growth, and the distance through which a planet migrates depends on the mass ejected from the system. Outward migration of Neptune carries that planet's MMRs outwards, leading to the sweep-up of KBOs (Malhotra 1995).

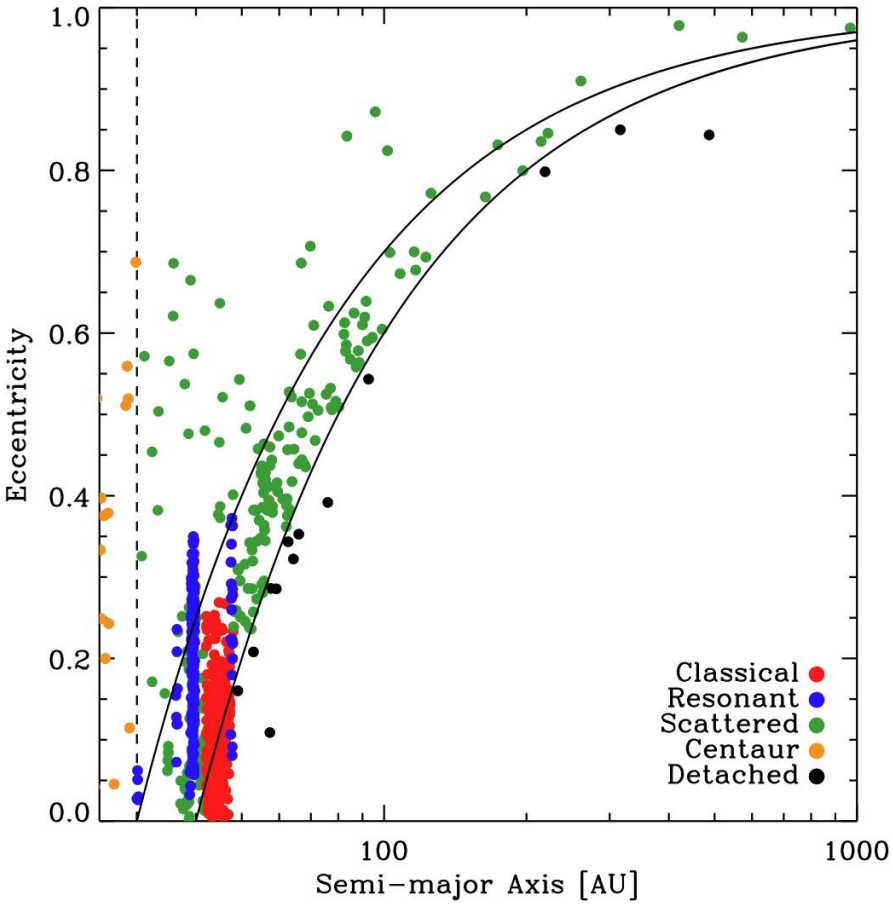


**Fig. 8** Same as Figure 7 but with a logarithmic x-axis extended to $a$ = 1000 AU to better show the extent of the scattered KBOs.

- Scattered Kuiper belt objects (green circles), also known as Scattered disk objects. These objects have typically eccentric and inclined orbits with perihelia in the $30 \leq q \leq 40$ AU range (Figures 7 and 8). The prototype is 1996 TL66, whose orbit stretches from ∼35 AU to ∼130 AU (Luu et al 1997). The brightness of these objects varies strongly around the orbit, such that a majority are visible only when near perihelion. For example, the survey in which 1996 TL66 was discovered lacked the sensitivity to detect the object over 88% of the orbital period. Accordingly, the estimated population is large, probably rivaling the rest of the Kuiper belt (Trujillo et al. 2001).
  Scattered KBOs owe their extreme orbital properties to continued, weak perihelic interactions with Neptune which excite the eccentricity to larger and larger values (Duncan and Levison 1997). The current aphelion record-holder is 87269 (2000 OO67) with $Q$ = 1123 AU. As the aphelion grows, so does the dynamical influence of external perturbations from passing stars and the asymmetric gravitational potential of the galactic disk.
- Detached Kuiper belt objects (black circles). The orbits of these bodies resemble those of the Scattered KBOs except that the perihelia are too far from Neptune, $q > 40$ AU, for planetary perturbations to have excited the eccentricities. The prototype is 2000 CR105, with $q$ = 44 AU (Gladman et al. 2002) but a more extreme example is the famous Sedna with $q$ = 74 AU (Brown et al. 2004).
  The mechanism by which the perihelia of the detached objects were lifted away from the influence of Neptune is unknown. The most interesting conjectures include the tidal action of external perturbers, whether they be unseen planets in our own system or unbound passing stars (Morbidelli and Levison 2004).

The Kuiper belt is a thick disk (Figure 9), with an apparent full width at half maximum, $FWHM \sim 10^\circ$ (Jewitt et al. 1996). The apparent width is an underestimate of the true width, however, because most KBOs have been discovered in surveys aimed near the ecliptic, and the sensitivity of such surveys varies inversely with the KBO inclination. Estimates of the unbiased (i.e. true) inclination distribution give $FWHM \sim 25$ to $30^\circ$ (Jewitt et al. 1996, Brown and Trujillo 2001, Elliot et al. 2005 - see especially Figure 20b). Moreover, all four components of the Kuiper belt possess broad inclination distributions (Figure 9). The inclination distribution of the Classical KBOs appears to be bimodal, with a narrow core superimposed on a broad halo (Brown and Trujillo 2001, Elliot et al. 2005).

The Kuiper belt is not thin like the Sun's original accretion disk and it is clear the the inclinations of the orbits of its members have been excited. The velocity dispersion amongst KBOs is $\Delta V$ = 1.7 km s$^{-1}$ (Jewitt et al. 1996, Trujillo et al. 2001). At these velocities, impacts between all but the largest KBOs lead to shattering and the production of dust, rather than to accretion and growth.

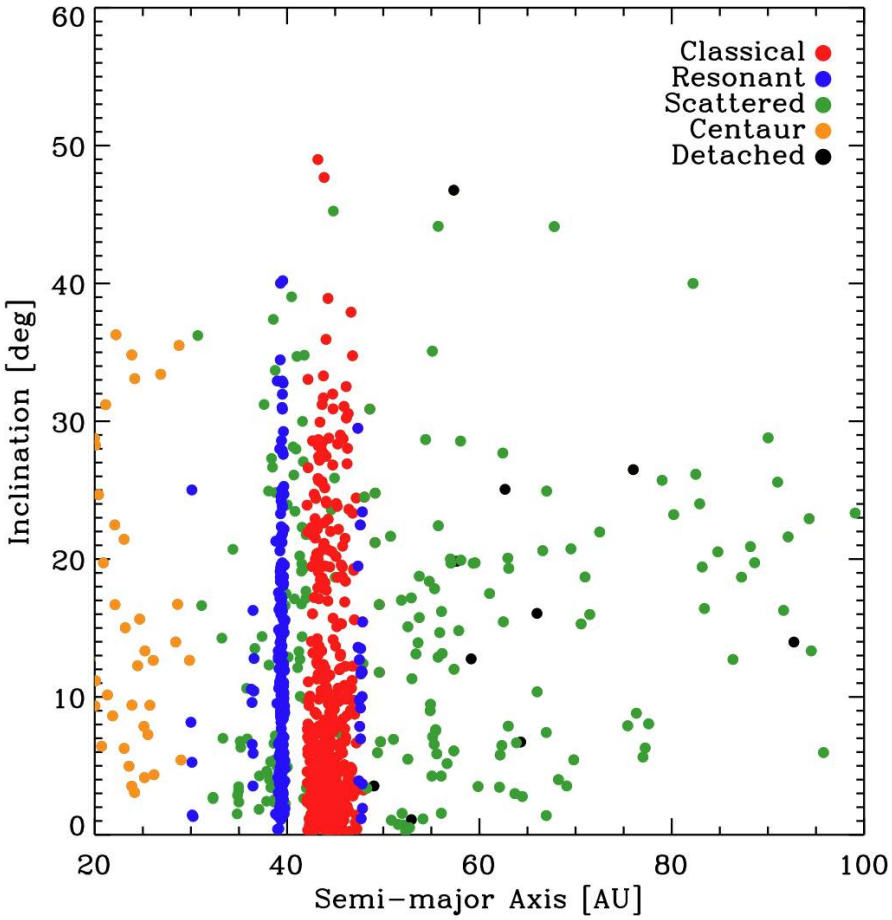


**Fig. 9** Orbital semimajor axis vs. inclination for KBOs known as of 2008 January 30. The plot shows that the KBOs occupy orbits having a wide range of inclinations. Most of the plotted objects were discovered in surveys directed towards the ecliptic, meaning that an observation bias *against* finding high inclination bodies is imprinted on the sample.

**Next generation** facilities should provide unprecedented survey capabilities (through *LSST*) that will provide a deep, all-sky survey of the Solar system to 24th visual magnitude, or deeper. The number of objects for which reliable orbits exist will increase from $\sim 10^3$, at present, by one to two orders of magnitude, depending on the detailed strategies employed by the surveys. Large samples are needed to assess the relative populations of the resonances and other dynamical niches that may place limits on the formation and evolution

of the OSS. Objects much larger than Pluto, perhaps in the Mars or Earth class, may also be revealed by careful work.

## 4 Interrelation of the Populations

Evidence that the small-body populations are interrelated is provided by dynamical simulations. The interrelations are of two basic types: a) those that occur through dynamical processes operating in the current Solar system and b) those that might have operated at an earlier epoch when the architecture of the Solar system may have been different from now.

As examples of the first kind, it is clear that objects in the Oort cloud and Kuiper belt reservoirs can be perturbed into planet crossing orbits, and that these perturbations drive a cascade from the outer Solar system through the Centaurs (bodies, asteroidal or cometary in nature) that are strongly interacting with the giant planets to the Jupiter family comets (orbits small enough for the Sun to initiate sublimation of near-surface ice and strongly interacting with Jupiter) to dead and dormant comets in the near-Earth "asteroid" population. In the current system, simulations show that it is *not* possible to capture the Trojans or the irregular satellites (Figure 11) of the giant planets from the passing armada of small bodies, and there is no known dynamical path linking comets from the Kuiper belt, for example, to comets in the main-belt (the MBCs).

The second kind of interrelation is possible because of planetary migration. The best evidence for the latter is deduced from the resonant Kuiper belt populations which, in one model, require that Neptune's orbit expanded by roughly 10 AU, so pushing its mean-motion resonances outwards through the undisturbed Kuiper belt (Malhotra 1995). The torques driving the migration moved Jupiter inwards (by a few $\times 0.1$ AU, since it is so massive) as the other giants migrated outwards. In one exciting model, the "Nice model", this migration pushed Jupiter and Saturn across the 2:1 mean motion resonance (Gomes et al. 2005). The dynamical consequences of the periodic perturbations induced between the Solar system's two most massive planets would have been severe (Figure 10). In published models, these perturbations excite a 30 $M_\oplus$ Kuiper belt, placing large numbers of objects into planet crossing orbits and clearing the Kuiper belt down to its current, puny mass of $\sim 0.1$ $M_\oplus$. During this clearing phase, numerous opportunities exist for trapping scattered KBOs in dynamically surprising locations. For example, the Trojans of the planets could have been trapped during this phase (Morbidelli et al. 2005). Some of the irregular satellites might likewise have been acquired at this time (Nesvorny et al. 2007; furthermore, any irregular satellites possessed by the planets *before* the mean-motion resonance crossing would have been lost). Other KBOs might have been trapped in the outer regions of the main-asteroid belt, perhaps providing a Kuiper belt source for ice in the MBCs.

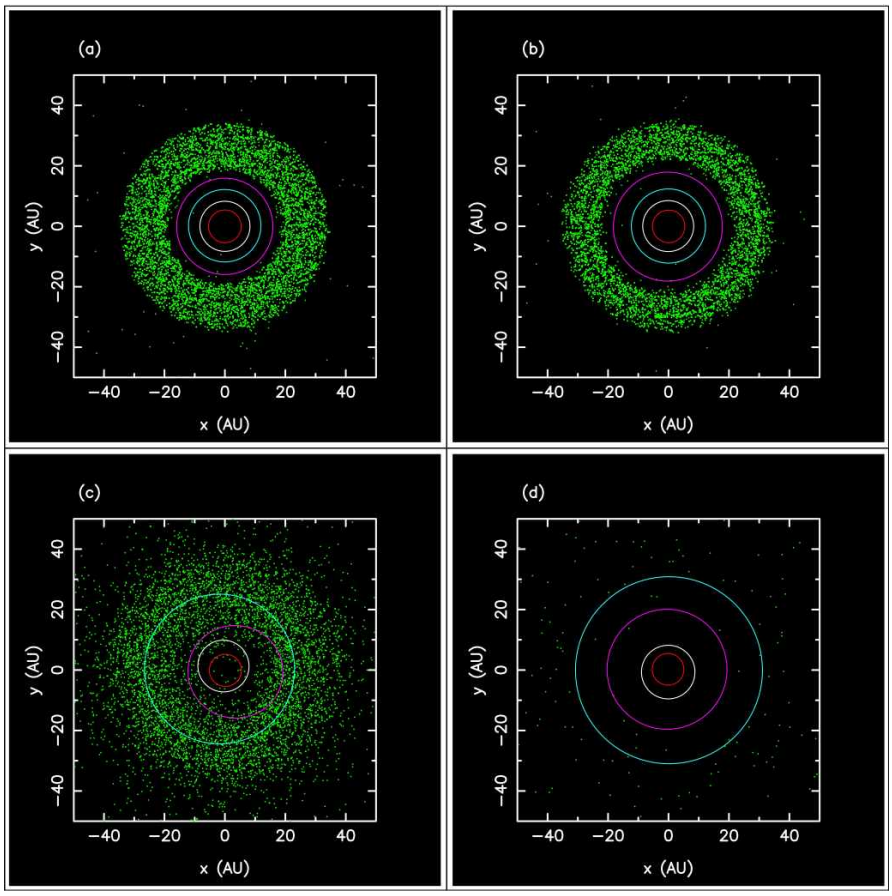


**Fig. 10** "Nice" model in which the architecture of the Solar system is set by the clearing of a massive (30 $M_{\oplus}$) Kuiper belt (stippled green region) when planets are thrown outwards by strong interactions between Jupiter (red) and Saturn (pink) at the 2:1 mean-motion resonance. (a) The initial configuration with the giant planets at 5.5, 8.2, 11.5 and 14.2 AU (b) Just before the 2:1 resonance crossing, timed to occur near 880 Myr from the start (c) 3 Myr after resonance crossing (note the large eccentricity of Uranus (purple) at this time and the placement of Neptune (blue) *in* the Kuiper belt) and (d) 200 Myr later, by which time the planetary orbits have assumed nearly their current properties. Adapted with permission from Gomes et al. 2005

Whether or not Jupiter and Saturn actually crossed the 2:1 resonance is unknown. In the Nice model, the 2:1 resonance crossing is contrived to occur at about 3.8 Gyr, so as to coincide with the epoch of the late-heavy bombardment (LHB). The latter is a period of heavy cratering on the Moon, thought by some to result from a sudden shower of impactors some 0.8 Gyr after the formation epoch. However, the interpretation of the crater age data is non-unique and reasonable arguments exist to interpret the LHB in other ways (Chapman et al. 2007). For example, the cratering

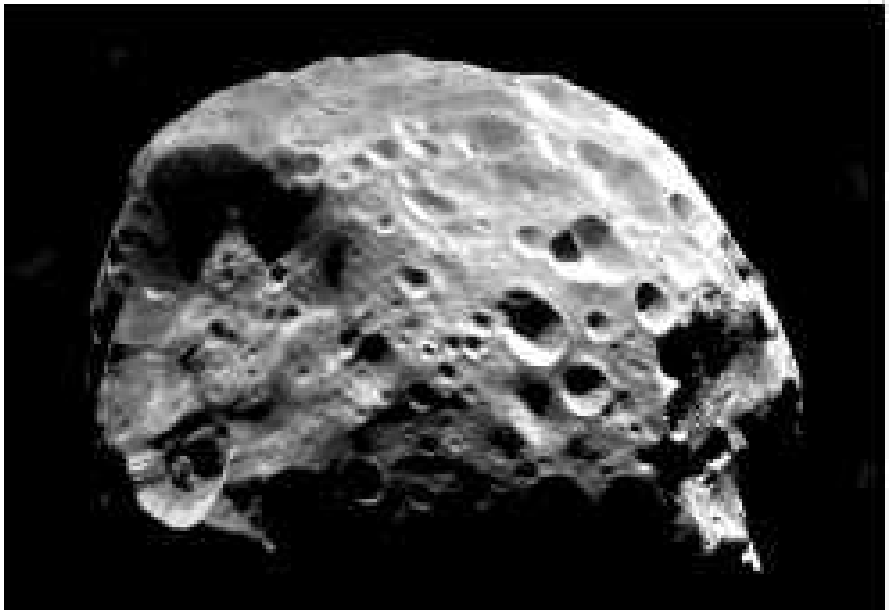

**Fig. 11** Saturn's irregular satellite Phoebe, which might be a captured Kuiper belt object. The effective spherical radius is $107\pm1$ km: the largest crater, Jason (at left), has a diameter comparable to the radius. The surface contains many ices (water, carbon dioxide) and yet is dark, with geometric albedo 0.08, as a consequence of dust mixed in the ice. Image from Cassini Imaging Team/NASA/JPL/Space Science Institute.

rate could merely *appear* to peak at 3.8 Gyr because all earlier (older) surfaces were destroyed by an impact flux even stronger than that at the LHB. (The LHB would then be an analog to the epoch in the expanding early universe when the optical depth first fell below unity and the galaxies became visible).

## 5 Evidence concerning the birth environment

Several lines of evidence suggest that the Sun was formed in a dense cluster.

The existence of widespread evidence for the decay products of short-lived isotopes in mineral inclusions in meteorites suggests that one or more supernovae exploded in the vicinity of the Sun, shortly before its formation. $^{26}$Al (half-life 0.7 Myr) was the first such unstable isotope to be identified (Lee et al. 1977) but others, like $^{60}$Fe (half-life 1.5 Myr) are known (and, unlike $^{26}$Al, cannot be produced by nuclear spallation reactions; Mostefaoui et al. 2004). It is possible, although not required, that the collapse formation of the protoplanetary nebula was triggered by

shock compression from the supernova that supplied the unstable nuclei (Ouellette et al. 2007).

The sharp outer edge to the classical Kuiper belt could be produced by a stellar encounter having an impact parameter $\sim$150 AU to 200 AU (Ida et al. 2000), although this is only one of several possible causes. Such close encounters are highly improbable in the modern epoch but would be more likely in the dense environment of a young cluster. At the same time, the survival and regularity of the orbits of the planets suggests that no very close encounter occurred (Gaidos 1995).

As noted above, the existence of a dense inner Oort cloud, required in some models to explain the source of the Halley family comets (long-period comets which include retrograde examples but which are not isotropically distributed), can only be populated via the stronger mean perturbations exerted between stars in a dense cluster.

Adams and Laughlin (2001) conclude from these and related considerations that the Sun formed in a cluster of $2000\pm1000$ stars.

## 6 Colors and Physical Properties

It has long been recognized that Kuiper belt objects exhibit a diversity in surface colors unparalleled among Solar system populations (Luu and Jewitt 1996). The distribution is relatively smooth from neutrally colored to extremely red objects. Indeed, a large fraction of KBOs (and Centaurs) is covered in "ultrared matter" (Jewitt 2002), the reddest material observed on small bodies. This material is absent in other populations, and is thought to be due to irradiated complex organics (Cruikshank et al. 2007). Further, the *UBVRIJ* colors are mutually correlated (Jewitt and Luu 1998; Jewitt et al. 2007), which seems to indicate that the spread is caused by a single reddening agent.

The wide range of colors suggests a broad range of surface compositions. However, such extreme non-uniformity in composition is unlikely to be intrinsic given the uniform and low temperatures across the disk of the Kuiper belt; the compositional spread is probably the result of some evolutionary process. Early theories to explain the color scatter invoke a competition between (the reddening) long-term exposure to cosmic radiation and (the de-reddening) impact resurfacing (Luu and Jewitt 1996; Delsanti et al. 2004), but the implied rotational color variability and correlation between color and collision likelihood are not observed (Jewitt and Luu 2001; Thébault and Doressoundiram 2003).

More recently it has been suggested that the diversity was emplaced when the small body populations were scattered by the outward migration of the ice giant planets (Gomes 2003), as a consequence of the mutual 2:1 resonance crossing by Jupiter and Saturn (see Nice model above). In other words, some of the objects now in the Kuiper belt may have formed much closer to the Sun, in the 10–20 AU region, where the chemistry would have been different and perhaps more diverse. Although appealing, the theory that the KB region was sprinkled with bodies from

various heliocentric distances remains a non-unique explanation and the implicit assumption that KBOs formed closer to the Sun should be less red remains ad-hoc. The relative importances of this dynamical mixing and the reddening effect by cosmic irradiation are still poorly understood. Cosmic-ray reddening seems to be important as the Classical KBOs, supposedly formed locally at 40 AU and having passively evolving surfaces only subject to cosmic radiation (their circular orbits protect them from mutual collisions), are on average the reddest KBOs (Tegler and Romanishin 2000).

A powerful way to investigate the physical properties of KBOs is by the analysis of their rotational properties, usually inferred from their lightcurves (Sheppard and Jewitt 2002; Lacerda and Luu 2006). Lightcurves are periodic brightness variations due to rotation: as a non-spherical (and non-azimuthally symmetric) KBO rotates in space, its sky-projected cross-section will vary periodically, and thus modulate the amount of sunlight reflected back to the observer. The period $P$ and range $\Delta m$ of a KBO's lightcurve provide information on its rotation period and shape, respectively. Multi-wavelength lightcurves may also reveal surface features such as albedo or color patchiness (Buie et al. 1992; Lacerda et al. 2008). These features are usually seen as second order effects superimposed on the principal, shape-regulated lightcurve. By combining the period and the range of a KBO lightcurve it is possible to constrain its density under the assumption that the object's shape is mainly controlled by its self-gravity (Jewitt and Sheppard 2002; Lacerda and Jewitt 2007). Lightcurves can also uncover unresolved, close binary objects (Sheppard and Jewitt 2004; Lacerda and Jewitt 2007).

Interesting KBOs, whose lightcurves have been particularly informative include: 1) 134340 Pluto, whose albedo-controlled light variations have been used to map the distribution of ices of different albedos across the surface (Buie et al. 1992; Young et al. 1999), which is likely controlled by the surface deposition of frosts from Pluto's thin atmosphere (Trafton 1989), 2) 20000 Varuna, whose rapid rotation ($P = 6.34 \pm 0.01$ hr) and elongated shape ($\Delta m = 0.42 \pm 0.03$ mag) indicate a bulk density $\rho \sim 1000$ kg m$^{-3}$ and hence require an internally porous structure (Jewitt and Sheppard 2002), 3) 139775 2001 QG298, whose extreme lightcurve (large range $\Delta m = 1.14 \pm 0.04$ mag and slow period $P \sim 13.8$ hr) suggests an extreme interpretation as a contact or near-contact binary (Sheppard and Jewitt 2004; Takahashi and Ip 2004; Lacerda and Jewitt 2007), and finally 4) 136198 2003 EL61, exhibiting super-fast rotation ($P = 3.9$ hr) that requires a density $\sim 2500$ kg m$^{-3}$, and a recently identified surface feature both redder and darker than the average surface (Lacerda et al. 2008).

Statistically, the rotational properties of KBOs can be used to constrain the distributions of spin periods (Lacerda and Luu 2006) and shapes (Lacerda and Luu 2003), which in turn can be used to infer the importance of collisions in their evolution. For instance, most main-belt asteroids have been significantly affected by mutual collisions, as shown by their quasi-Maxwellian spin rate distribution (Harris 1979; Farinella et al. 1981) and a shape distribution consistent with fragmentation experiments carried out in the laboratory (Catullo et al. 1984). KBOs spin on average more slowly ($\langle P_{KBO} \rangle \sim 8.4$ hr vs. $\langle P_{ast} \rangle \sim 6.0$ hr; Lacerda and Luu 2006) and are more spherical (as derived from the $\Delta m$ distribution; Luu and Lacerda 2003; Sheppard

et al. 2008) than asteroids of the same size, both indicative of a milder collisional history. Typical impact speeds in the current Kuiper belt and main asteroid belt are respectively 2 and 5 km $s^{-1}$. However, three of the four KBOs listed in the previous paragraph show extreme rotations and shapes, likely the result of collision events. Because the current number density of KBOs is too low for these events to occur on relevant timescales, their rotations were probably aquired at an early epoch when the Kuiper belt was more massive and collisions were more frequent (Davis and Farinella 1997; Jewitt and Sheppard 2002).

**Next generation** telescopes will provide revolutionary new data on the physical properties of KBOs. Their colors and rotational properties can potentially reveal much about these objects' surface and physical natures. *JWST*, in particular, will provide high quality near-infrared spectra that will place the best constraints on the (probably) organic mantles of the KBOs, thought to be some of the most primitive matter in the Solar system. Separate measurements of the albedos and diameters, obtained from optical/thermal measurements using *ALMA* and *JWST*, will give the albedos and accurate diameters, needed to fully understand the surface materials.

Survey data will permit the identification of $>$100 wide binaries, while the high angular resolution afforded by *JWST* will reveal a much larger number (thousands?) of close binaries. Orbital elements for each will lead to the computation of system masses through Kepler's law. Diameters from optical/thermal measurements (using *ALMA* and *JWST*) will then permit the determination of system densities for KBOs over a wide range of diameters and orbital characteristics in the Kuiper belt. Density, as the "first geophysical parameter", provides our best handle on accretion models of the Kuiper belt objects.

## 7 Solar System Dust

Collisions between solids in the early Solar system generally resulted in agglomeration due to the prevailing low impact energies. However, at present times, high impact energies dominate and collisions result in fragmentation and the generation of dust from asteroids, comets and KBOs. Due to the effect of radiation forces (see § 7.2) these dust particles spread throughout the Solar system forming a dust disk.

## *7.1 Inner Solar System: Asteroidal and Cometary Dust*

The existence of dust in the inner Solar system (a.k.a. Zodiacal cloud) has long been known since the first scientific observations of the Zodiacal light by Cassini in 1683, correctly interpreted by de Duiliers in 1684 as produced by sunlight reflected from small particles orbiting the Sun. Other dust-related phenomena that can be observed naked eye are dust cometary tails and "shooting stars".

The sources of dust in the inner Solar system are the asteroids, as evident from the observation of dust bands associated with the recent formation of asteroidal families, and comets, as evident from the presence of dust trails and tails. Their relative contribution can be studied from the He content of collected interplanetary dust particles, which is strongly dependent on the velocity of atmospheric entry, expected to be low for asteroidal dust and high for cometary dust. Their present contributions are thought to differ by less than a factor of 10 (Brownlee et al. 1994), but they have likely changed with time. It is thought that due to the depletion of asteroids, the asteroidal dust surface area has slowly declined by a factor of 10 (Grogan et al. 2001) with excursions in the dust production rate by up to an order of magnitude associated with breakup events like those giving rise to the Hirayama asteroid families that resulted in the formation of the dust bands observed by *IRAS* (Sykes and Greenberg 1986). The formation of the Veritas family 8.3 Myr ago still accounts for $\sim$25% of the Zodiacal thermal emission today (Dermott et al. 2002). A major peak of dust production in the inner Solar system is expected to have occurred at the time of the LHB (§4), as a consequence of an increased rate of asteroidal collisions and to the collisions of numerous impactors originating in the main asteroid belt (Strom et al. 2005) with the terrestrial planets.

The thermal emission of the Zodiacal cloud dominates the night sky between 5–500 $\mu$m and has a fractional luminosity of $L_{dust}/L_{Sun} \sim 10^{-8}$–$10^{-7}$ (Dermott et al. 2002). Studied by *IRAS*, *COBE* and *ISO* space telescopes, it shows a featureless spectrum produced by a dominant population of low albedo ($<$0.08) rapidly-rotating amorphous forsterite/olivine grains that are 10–100 $\mu$m in size and are located near 1 AU. The presence a weak (6% over the continuum) 10 $\mu$m silicate emission feature indicates the presence of a small population of $\sim$1 $\mu$m grains of dirty crystalline olivine and hydrous silicate composition (Reach et al. 2003).

Interplanetary dust particles (IDPs) have been best characterized at around 1 AU by in situ satellite measurements, observations of micro-meteorite impact craters on lunar samples, ground radar observations of the ionized trails created as the particles pass through the atmosphere and laboratory analysis of dust particles collected from the Earth's stratosphere, polar ice and deep sea sediments. Laboratory analysis of collected IDPs show that the particles are 1–1000$\mu$m in size, typically black, porous ($\sim$40%) and composed of mineral assemblages of a large number of submicron-size grains with chondritic composition and bulk densities of 1–3 g/cm$^3$. Their individual origin, whether asteroidal or cometary, is difficult to establish. The cumulative mass distribution of the particles at 1 AU follows a broken power-law such that the dominant contribution to the cross sectional area (and therefore to the zodiacal emission) comes from $10^{-10}$ kg grains ($\sim$30 $\mu$m in radius), while the dom-

inant contribution to the total dust mass comes from $\sim 10^{-8}$ kg grains (Leinert and Grün 1990).

In situ spacecraft detections of Zodiacal dust out to 3 AU, carried out by Pioneer 8–11, Helios, Galileo and Ulysses, showed that the particles typically have $i < 30^{\circ}$ and $e > 0.6$ with a spatial density falling as $r^{-1.3}$ for $r < 1$ AU and $r^{-1.5}$ for $r > 1$ AU, and that there is a population of grains on hyperbolic orbits (a.k.a $\beta$-meteoroids), as well as stream of small grains origina jovian system (see review by Grün et al. 2001).

## *7.2 Outer Solar System: Kuiper Belt Dust*

As remarked above, collisions in the modern-day Kuiper belt are erosive, not agglomerative, and result in the production of dust. In fact, two components to Kuiper belt dust production are expected: (1) erosion of KBO surfaces by the flux of interstellar meteoroids (e.g. Grün et al. 1994), leading to the steady production of dust at about $10^3$ to $10^4$ kg s$^{-1}$ (Yamamoto and Mukai 1998); and (2) mutual collisions between KBOs, with estimated dust production of about (0.01–3)$\times 10^8$ kg s$^{-1}$ (Stern 1996). For comparison, the dust production rate in the Zodiacal cloud, from comets and asteroids combined, is about $10^3$ kg s$^{-1}$ (Leinert et al. 1983). The fractional luminosity of the KB dust is expected to be around $L_{dust}/L_{Sun} \sim 10^{-7}$–$10^{-6}$ (Stern 1996), compared to $L_{dust}/L_{Sun} \sim 10^{-8}$–$10^{-7}$ for the Zodiacal cloud (Dermott et al. 2002).

Observationally, detection of Kuiper belt dust at optical wavelengths is confounded by the foreground presence of cometary and asteroidal dust in the Zodiacal cloud. Thermally, these near and far dust populations might be distinguished on the basis of their different temperatures ($\sim$200 K in the Zodical cloud vs. $\sim$40 K in the Kuiper belt) but, although sought, Kuiper belt dust has not been detected this way (Backman et al. 1995). At infrared thermal wavelengths both foreground Zodiacal cloud dust *and* background galactic dust contaminate any possible emission from Kuiper belt dust. The cosmic microwave background radiation provides a very uniform source against which emission from the Kuiper belt might potentially be detected but, again, no detection has been reported (Babich et al. 2007).

Whereas remote detections have yet to be achieved, the circumstances for in-situ detection are much more favorable (Gurnett et al. 1997). The Voyager 1 and 2 plasma wave instruments detected dust particles via the pulses of plasma created by high velocity impacts with the spacecraft. Because the plasma wave detector was not built with impact detection as its primary purpose, the properties and flux of the impacting dust are known only approximately. Still, several important results are available from the Voyager spacecraft. Impacts were recorded continuously as the Voyagers crossed the (then unknown) Kuiper belt region of the Solar system. The smallest dust particles capable of generating measurable plasma are thought to be $a_0 \sim 2$ $\mu$m in radius. Measured in the 30 AU to 60 AU region along the Voyager flight paths, the number density of such particles is $N_1 \sim 2\times 10^{-8}$ m$^{-3}$. Taking the

thickness of the Kuiper belt (measured perpendicular to the midplane) as $H \sim 10$ AU, this corresponds to an optical depth $\tau \sim \pi a_0^2 H N_1 \sim 4 \times 10^{-7}$, roughly $10^3$ times smaller than the optical depth of a $\beta$-Pictoris class dust circumstellar disk. An upper limit on the density of gravel (*cm*-sized) particles in the Kuiper belt is provided by the survival of a 20-cm propellant tank on the Pioneer 10 spacecraft (Anderson et al. 1998).

## *7.3 Dust Dynamics and Dust Disk Structure*

After the dust particles are released from their parent bodies (asteroids, comets and KBOs) they experience the effects of radiation and stellar wind forces. Due to radiation pressure, their orbital elements and specific orbital energy change immediately upon release. If their orbital energy becomes positive ($\beta > 0.5$), the dust particles escape on hyperbolic orbits (known as $\beta$-meteoroids – Zook & Berg 1975). If their orbital energy remains negative ($\beta < 0.5$), their semi-major axis increases but they remain on bound orbits. Their new semimajor axis and eccentricity $(a', e')$ in terms of that of their parent bodies ($a$ and $e$) are $a' = a\frac{1-\beta}{1-2a\beta/r}$ and $e' = \mid 1 - \frac{(1-2a\beta/r)(1-e^2)}{(1-\beta^2)} \mid^{1/2}$ (their inclination does not change), where $r$ is the particle location at release and $\beta$ is the ratio of the radiation pressure force to the gravitational force. For spherical grains orbiting the Sun, $\beta = 5.7 Q_{pr}/\rho b$, where $\rho$ and $b$ are the density and radius of the grain in MKS units and $Q_{pr}$ is the radiation pressure coefficient, a measure of the fractional amount of energy scattered and/or absorbed by the grain and a function of the physical properties of the grain and the wavelength of the incoming radiation (Burns, Lamy & Soter 1979).

With time, Poynting-Rorbertson (P-R) and solar wind corpuscular drag (which result from the interaction of the dust grains with the stellar photons and solar wind particles, respectively) tend to circularize and decrease the semimajor axis of the orbits, forcing the particles to slowly drift in towards the central star until they are destroyed by sublimation in a time given by $t_{PR} = 0.7(\frac{b}{\mu m})(\frac{\rho}{kg/m^3})(\frac{R}{AU})^2(\frac{L_\odot}{L_*})\frac{1}{1+albedo}\ yr$, where $R$ is the starting heliocentric distance of the dust particle and $b$ and $\rho$ are the particle radius and density, respectively (Burns, Lamy and Soter 1979 and Backman and Paresce 1993). If the dust is constantly being produced from a planetesimal belt, and because the dust particles inclinations are not affected by radiation forces, this inward drift creates a dust disk of wide radial extent and uniform density. Grains can also be destroyed by mutual grain collisions, with a collisional lifetime of $t_{col} = 1.26 \times 10^4 (\frac{R}{AU})^{3/2}(\frac{M_\odot}{M_*})^{1/2}(\frac{10^{-5}}{L_{dust}/L_*})yr$ (Backman and Paresce 1993).

For dust disks with $M_{dust} > 10^{-3}\ M_\oplus$, $t_{col} < t_{PR}$, i.e. the grains are destroyed by multiple mutual collisions before they migrate far from their parent bodies (in this context, "destruction" means that the collisions break the grains into smaller and smaller pieces until they are sufficiently small to be blown away by radiation pressure). This regime is referred to as collision-dominated. The present Solar system,

however, is radiation-dominated because it does not contain large quantities of dust and $t_{col} > t_{PR}$, i.e. the grains can migrate far from the location of their parent bodies. This is particularly interesting in systems with planets and outer dust-producing planetesimal belts because in their journey toward the central star the orbits of the dust particles are affected by gravitational perturbations with the planets via the trapping of particles in mean motion resonances (MMRs), the effect of secular resonances and the gravitational scattering of dust. This results in the formation of structure in the dust disk (Figure 12).

Dust particles drifting inward can become entrapped in exterior MMRs because at these locations the particle receives energy from the perturbing planet that can balance the energy loss due to P-R drag, halting the migration. This makes the lifetime of particles trapped in outer MMRs longer than in inner MMRs (Liou & Zook 1997), with the former dominating the disk structure. This results in the formation of resonant rings outside the planet's orbit, as the vast majority of the particles spend most of their lifetimes trapped in exterior MMRs. In some cases, due to the geometry of the resonance, a clumpy structure is created. Figure 12 (from Moro-Martín and Malhotra 2002) shows the effect of resonant trapping expected in the (yet to be observed) KB dust disk, where the ring-like structure, the asymmetric clumps along the orbit of Neptune, and the clearing of dust at Neptune's location are all due to the trapping of particles in MMRs with Neptune (as seen in the histogram of semimajor axis). Neptune plays the leading role in the trapping of dust particles because of its mass and because it is the outermost planet and its exterior resonances are not affected by the interior resonances from the other planets. Trapping is more efficient for larger particles (i.e. smaller $\beta$ values) because the drag force is weaker and the particles cross the resonance at a slower rate increasing their probability of being captured. The effects of resonance trapping in hypothetical planetary systems each consisting of a single planet on a circular orbit and an outer planetesimal belt similar to the KB are shown in Figure **??**. More eccentric planets ($e < 0.6$) can also create clumpy eccentric rings and offset rings with a pair of clumps (Kuchner and Holman 2003). Even though, as mentioned in §7.2, the KB dust disk has yet to be observed, this is not the case for the Zodical cloud, for which *IRAS* and *COBE* thermal observations show that there is a ring of asteroidal dust particles trapped in exterior resonances with the Earth at around 1 AU, with a 10% number density enhancement on the Earth's wake that results from the resonance geometry (Dermott et al. 1994).

Secular perturbations, the long-term average of the perturbing forces, act on timescales $>$0.1 Myr. If the planet and the planetesimal disk are not coplanar, the secular perturbations can create a warp in the dust disk as their tendency to align the orbits operates on shorter timescales closer to the star. A warp can also be created in systems with two non-coplanar planets. If the planet is in an eccentric orbit, the secular resonances can force an eccentricity on the dust particles and this creates an offset in the disk center with respect to the star that can result in a brightness asymmetry. Other effects of secular perturbations are spirals and inner gaps (Wyatt et al. 1999). The effect of secular perturbations can be seen in *IRAS* and *COBE* observations on the Zodiacal cloud and account for the presence of an inner edge around

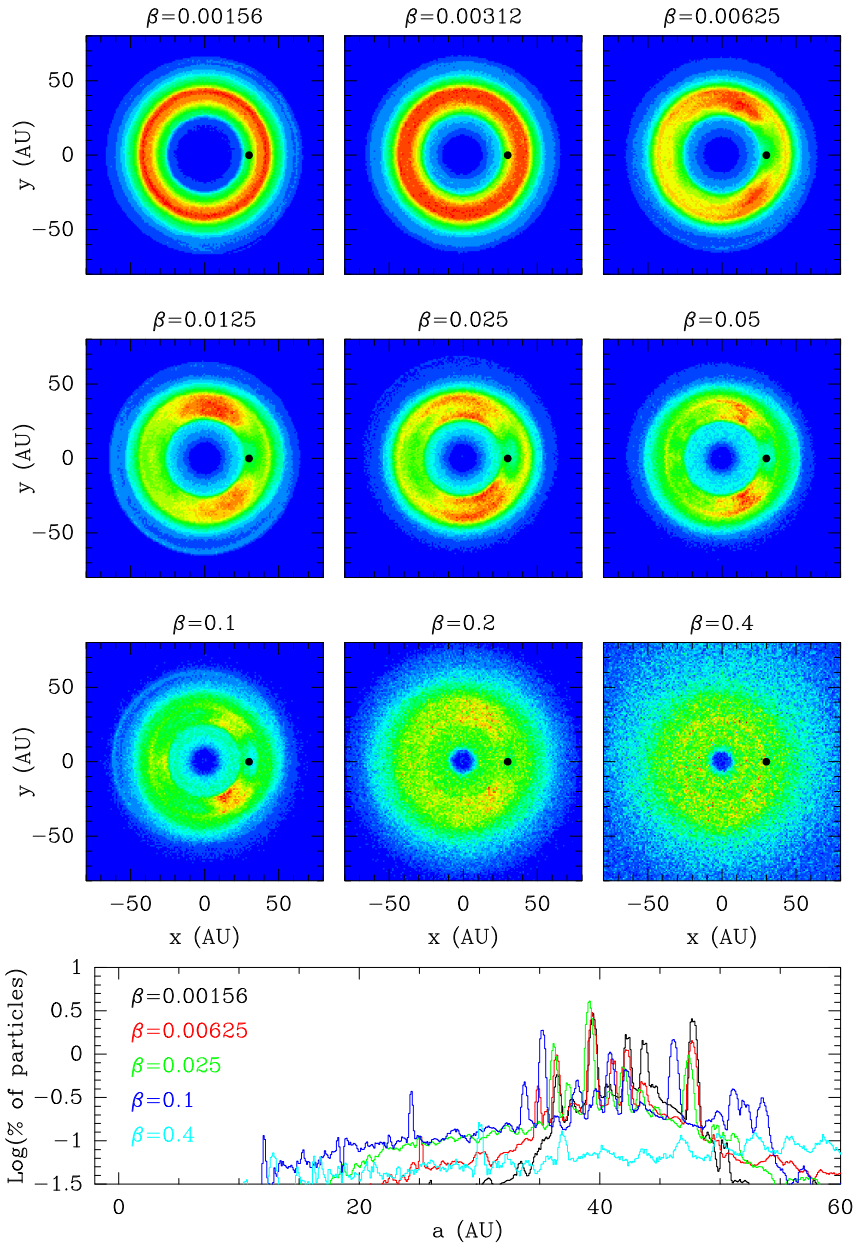


**Fig. 12** Expected number density distribution of the KB dust disk for nine different particle sizes (or $\beta$ values). $\beta$ is a dimensionless constant equal to the ratio between the radiation pressure force and the gravitational force and depends on the density, radius and optical properties of the dust grains. If we assume that the grains are composed of spherical astronomical silicates ($\rho$=2.5, Weingartner & Draine 2001), $\beta$ values of 0.4, 0.2, 0.1, 0.05, 0.025, 0.0125, 0.00625, 0.00312, 0.00156 correspond to grain radii of 0.7, 1.3, 2.3, 4.5, 8.8, 17.0, 33.3, 65.9, 134.7 $\mu$m, respectively. The trapping of particles in MMRs with Neptune is responsible for the ring-like structure, the asymmetric clumps along the orbit of Neptune, and the clearing of dust at Neptune's location (indicated with a black dot). The disk structure is more prominent for larger particles (smaller $\beta$ values) because the P-R drift rate is slower and the trapping is more efficient. The disk is more extended in the case of small grains (large $\beta$ values) because small particles are more strongly affected by radiation pressure. The histogram shows the relative occurrence of the different MMRs for different sized grains, where the large majority of the peaks correspond to MMRs with Neptune. The inner depleted region inside $\sim$ 10 AU is created by gravitational scattering of dust grains with Jupiter and Saturn. More details on these models can be found in Moro-Martín & Malhotra (2002, 2003).

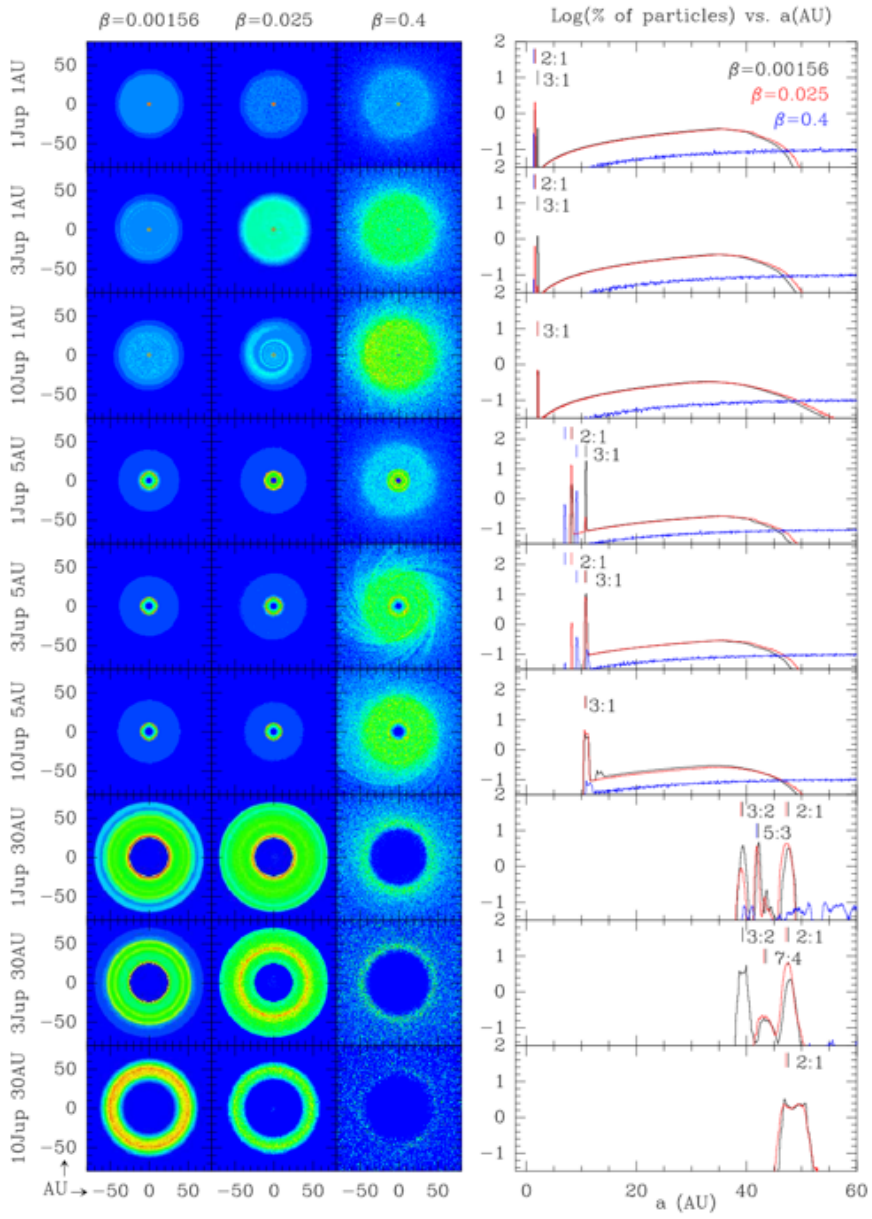


**Fig. 13** Same as Figure 12 but for nine hypothetical planetary systems around a solar type star consisting of a single planet with a mass of 1, 3 or 10$M_{Jup}$ in a circular orbit at 1, 5 or 30 AU, and a coplanar outer planetesimal belt similar to the KB. The models with 1 $M_{Jup}$ planet at 1 and 5 AU show that the dust particles are preferentially trapped in the 2:1 and 3:1 resonances, but when the mass of the planet is increased to 10 $M_{Jup}$, and consequently the hill radius of the planet increases, the 3:1 becomes dominant. The resonance structure becomes richer when the planet is further away from the star, and when the mass of the planet decreases (compare the model for a 1$M_{Jup}$ planet at 30 AU with the Solar system model in Figure 12, where the structure is dominated by Neptune). From Moro-Martín, Wolf & Malhotra (in preparation).

2 AU due to a secular resonance with Saturn (that also explains the inner edge of the main asteroid belt), the offset of the cloud center with respect to the Sun, the inclination of the cloud with respect to the ecliptic, and the cloud warp (see review in Dermott et al. 2001).

The efficient ejection of dust grains by gravitational scattering with massive planets as the particles drift inward from an outer belt of planetesimals (Figures 14 and 15) can result in the formation of a dust depleted region inside the orbit of the planet (Figures 12 and 13), such as the one expected inside 10 AU in the KB dust disk models (due to gravitational scattering by Jupiter and Saturn).

**Next generation** facilities will probably be unable to detect diffuse emission from Kuiper dust because the optical depth is so low, and the effects of foreground and background confusion so large. However, small Kuiper belt objects are sufficiently numerous that there is a non-negligible chance that the collision clouds of recent impacts will be detected (Stern 1996). Such clouds can potentially be very bright, and evolve on timescales (days and weeks) that are amenable to direct observational investigation using *LSST* and *JWST*. Collision cloud measurements provide our best chance to understand the sub-kilometer population in the Kuiper belt. These objects are too small to be directly detected but are of special relevance as the precursors to the Centaurs and Jupiter family comet nuclei. Measurement of their number is of central importance in understanding the role of the Kuiper belt as the JFC source, and as the source of Kuiper dust.

## 8 Kuiper Belts of Other Stars

Radial velocity studies have revealed that $>7\%$ of solar-type stars harbor giant planets with masses $<13$ $M_{Jup}$ and semimajor axis $<$ 5 AU (Marcy et al. 2005). This is a lower limit because the duration of the surveys (6–8 years) limits the ability to detect planets long-period planets; the expected frequency extrapolated to 20 AU is $\sim 12\%$ (Marcy et al. 2005). As of February 2008, 276 extra-solar planets have been detected with a mass distribution that follows $dN/dM \propto M^{-1.05}$ from $0.3 M_{Jup}$ to 10 $M_{Jup}$ (the surveys are incomplete at smaller masses). A natural question arises whether these planetary systems, some of them harboring multiple planets, also contain planetesimals like the asteroids, comets and KBOs in the Solar system. Long before extra-solar planets were discovered we inferred that the answer to this question was yes: colliding planetesimals had to be responsible for the dust disks observed around mature stars. In §8.1 we will discuss how these dust disks, known as *debris disks*, can help us study indirectly Kuiper belts around other stars; other methods by which extra-solar Kuiper belts might be found and characterized in the future will be discussed in §8.2 and §8.3.

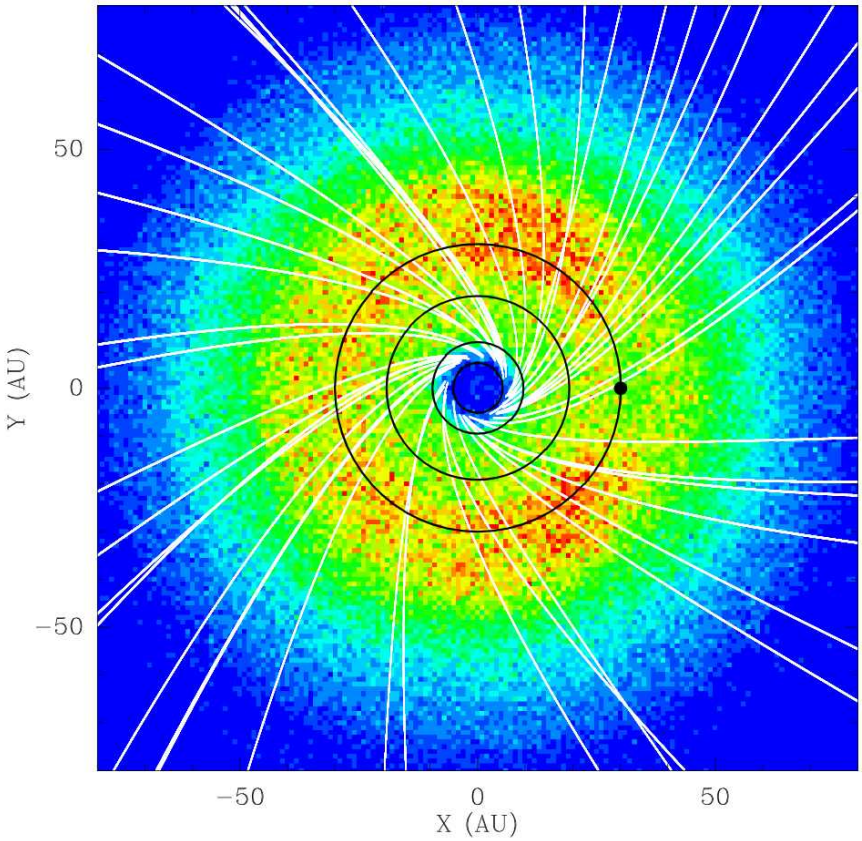


**Fig. 14** Expected number density distribution of a KB dust disk composed of particles with $\beta$ = 0.2 with the trajectories of the particles ejected by Jupiter in white. The black dot indicates the position of Neptune and the circles correspond to the orbits of the Giant planets. In addition to the population of small grains with $\beta > 0.5$ blown-out by radiation pressure, the gravitational scattering by the giant planets (Jupiter and Saturn in the case of the Solar system) produces an outflow of large grains ($\beta < 0.5$) that is largely confined to the ecliptic (Moro-Martín & Malhotra 2005b). Interestingly, a stream of dust particles arriving from the direction of $\beta$ Pictoris has been reported by Baggaley (2000).

## *8.1 Debris Disks*

### 8.1.1 Evidence of Planetesimals

Theory and observations show that stars form in circumstellar disks composed of gas and dust that had previously collapsed from the densest regions of molecular clouds. For solar type stars, the masses of these disks are $\sim$ 0.01–0.10 $M_\odot$ and ex-

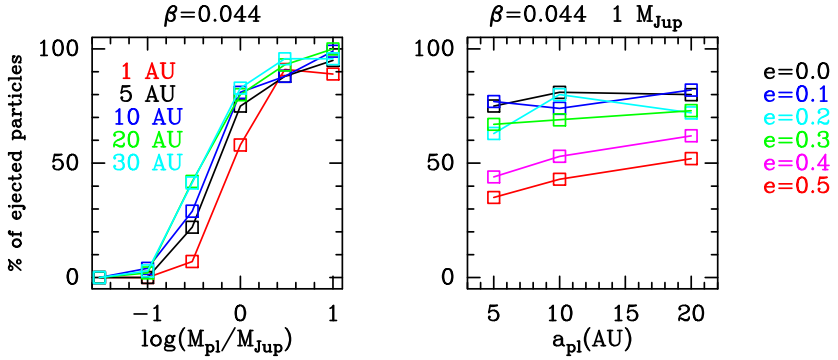


**Fig. 15** Percentage of dust particles ejected from the system by gravitational scattering with the planet for the single planet models in Figure 13. The particle size is fixed, corresponding to grains with $\beta = 0.044$. Because gravitational scattering is independent of the particle size, the efficiency of ejection is fairly independent of $\beta$. *Left*: Dependency of the efficiency of ejection on the planet's mass (x-axis) and the planet's semimajor axis (indicated by the different colors). *Right*: Dependency of the efficiency of ejection on the planet semimajor axis (x-axis) and eccentricity (corresponding to the different colors). The models in the right panel correspond to a 1 $M_{Jup}$ mass planet on a circular orbit around a solar type star. Planets with masses of 3–10 $M_{Jup}$ at 1 AU–30 AU in a circular orbit eject >90% of the dust grains that go past their orbits under P-R drag; a 1 $M_{Jup}$ planet at 30 AU ejects >80% of the grains, and about 50%–90% if located at 1 AU, while a 0.3 $M_{Jup}$ planet is not able to open a gap, ejecting < 10% of the grains. These results are valid for dust grains sizes in the range 0.7 $\mu$m–135 $\mu$m. From Moro-Martín and Malhotra 2005.

tend to 100s of AU, comparable to the minimum mass solar nebula ($\sim$0.015 $M_\odot$ , which is the mass required to account for the condensed material in the Solar system planets). Over time, these primordial or proto-planetary disks, with dust grain properties similar to those found in the interstellar medium, dissipate as the disk material accretes onto the star, is blown away by stellar wind ablation, photo-evaporation or high-energy stellar photons, or is stripped away by passing stars. The primordial gas and dust in these disks dissipate in less than $10^7$ years (see e.g. Hartmann 2000 and references therein).

However, it is found that some main sequence stars older than $\sim 10^7$ years show evidence of dust emission. In most cases, this evidence comes from the detection of an infrared flux in excess of that expected from the stellar photosphere, thought to arise from the thermal emission of circumstellar dust. In some nearby stars, like the ones shown in Figures 16, 17 and 18, direct imaging has confirmed that the emission comes from a dust disk. In §7.3 we discussed the lifetimes of the dust grains due to radiation pressure, P-R drag and mutual grain collisions. It is found that in most cases these lifetimes are much shorter than the age of the star[1], and therefore the

[1] One needs to be cautious with this argument because the ages of main sequence stars are difficult to determine. For example, the prototype (and best studied) of debris disk $\beta$-Pictoris, was dated at $\sim$100 to 200 Myr (Paresce 1991) but later become only $\sim$20 Myr old (Barrado y Navascués et al. 1999).

observed dust cannot be primordial but is more likely produced by a reservoir of undetected dust-producing planetesimals, like the KBOs, asteroids and comets in the Solar system (see e.g. Backman and Paresce 1993). This is why these dust disks observed around mature main sequence stars are known as debris disks. Debris disks are evidence of the presence of planetesimals around other main sequence stars. In the core accretion model, these planetesimals formed in the earlier protoplanetary disk phase described above, as the ISM-like dust grains sedimented into the mid-plane of the disk and aggregated into larger and larger bodies (perhaps helped by turbulence) until they became planetesimals, the largest of which could potentially become the seeds out of which the giant planets form from the accretion of gas onto these planetary cores.

Even though these extra-solar planetesimals remain undetected, the dust they produce has a much larger cumulative surface area that makes the dust detectable in scattered light and in thermal emission. The study of these debris disks can help us learn indirectly about their parent planetesimals, roughly characterizing their frequencies, location and composition, and even the presence of massive planets.

### 8.1.2 Spatially Resolved Observations

Most debris disk observations are spatially unresolved and the debris disks are identified from the excess thermal emission contributed by dust in their spectral energy distributions (SEDs). In a few cases (about two dozen so far), the disks are close enough and the images are spatially resolved. Figures 16, 17 and 18 show the most spectacular examples. These high resolution observations show a rich diversity of morphological features including warps (Au-Mic & $\beta$-Pic), offsets of the disk center with respect to the central star ($\varepsilon$-Eri and Fomalhaut), brightness asymmetries (HD 32297 and Fomalhaut), clumpy rings (Au-Mic, $\beta$-Pic, $\varepsilon$-Eri and Fomalhaut) and sharp inner edges (Fomalhaut), features that, as discussed in §7.3 could be due to gravitational perturbations of massive planets, and that in some cases have been observed in the zodiacal cloud, while in other cases used to belong to the realm of KB disk models. Even though the origin of individual features is still under discussion and the models require further refinements (e.g. in the dust collisional processes and the effects of gas drag), the complexity of these features, in particular the azimuthal asymmetries, indicate that planets likely play a role in the creation of structure in the debris disks. This is of interest because the structure, in particular that created by the trapping of particles in MMRs, is sensitive to the presence of moderately massive planets at large distances (recall the KB dust disk models and the structure created by Neptune). This is a parameter space that cannot be explored with the present planet detection techniques, like the radial velocity and transient studies, and therefore the study of debris disk structure can help us learn about the diversity of planetary systems. In this context, high resolution debris disk observations over a wide wavelength range are of critical importance, like those to be obtained with *Herschel*, *JWST* and *ALMA*.

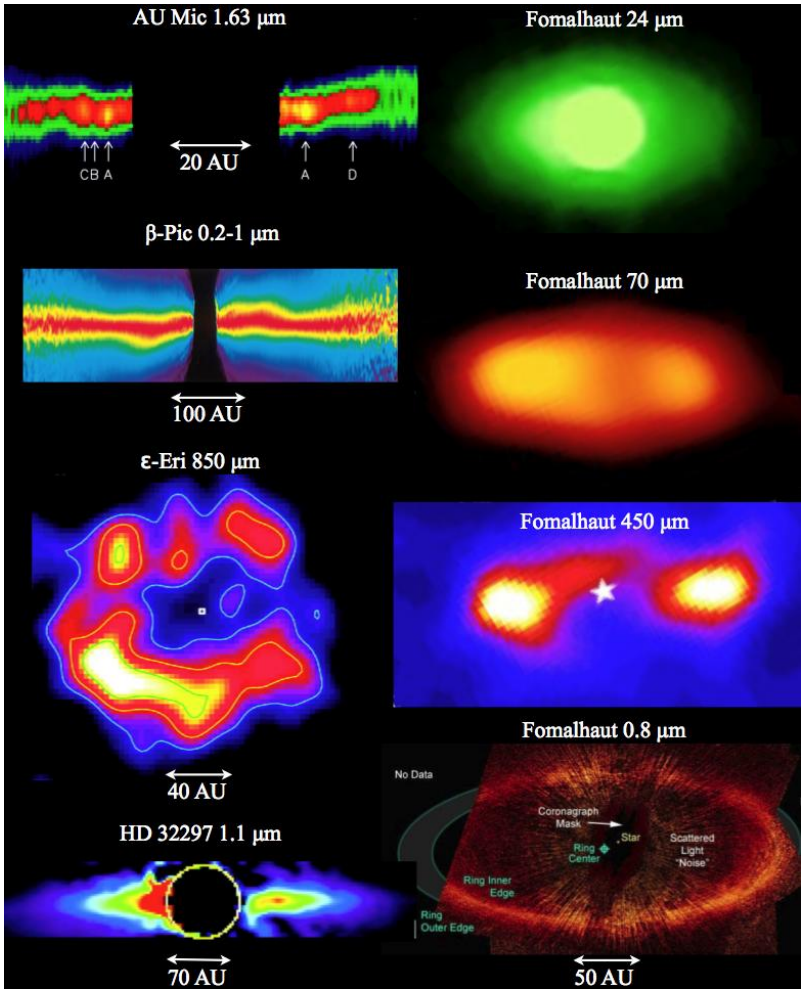


**Fig. 16** Spatially resolved images of nearby debris disks showing dust emission from 10s to 100s of AU with a wide diversity of complex features including inner gaps, warps, brightness asymmetries, offsets and clumply rings, some of which may be due to the presence of massive planets (§7.3). *Left* (from top to bottom): AU-Mic (Keck AO at 1.63 $\mu$m; Liu 2004), $\beta$-Pic (STIS CCD coronography at 0.2–1 $\mu$m; Heap et al. 2000), $\epsilon$-Eri (JCMT/SCUBA at 850 $\mu$m; Greaves et al. 2005) and HD 32297 (HST/NICMOS coronography at 1.1 $\mu$m; Schneider, Silverstone and Hines 2005). *Right*. All images correspond to Fomalhaut (7.7 pc away) and are on the same scale. From top to bottom: Spitzer/MIPS at 24 $\mu$m (Stapelfeldt et al. 2004); Spitzer/MIPS at 70 $\mu$m (Stapelfeldt et al. 2004); JCMT/SCUBA at 450 $\mu$m (Holland et al. 2003) and HST/ACS at 0.69–0.97 $\mu$m (Kalas et al. 2005). For this last panel, the annular disk in the scattered light image has an inner radius of $\sim$133 AU and a radial thickness of $\sim$25 AU and its center is offset from the star by about 15$\pm$1 AU in the plane, possibly induced by an unseen planet. Its sharp inner edge has also been interpreted as a signature of a planet (Kalas et al. 2005). The dust mass of the Fomalhaut debris disk in millimeter-sized particles is about $10^{23}$ kg ($\sim$0.02 $M_\oplus$; Holland et al. 1998) but, if larger bodies are present, the mass could be 50 to 100 $M_\oplus$, or about 1000 times the mass of our Kuiper belt.

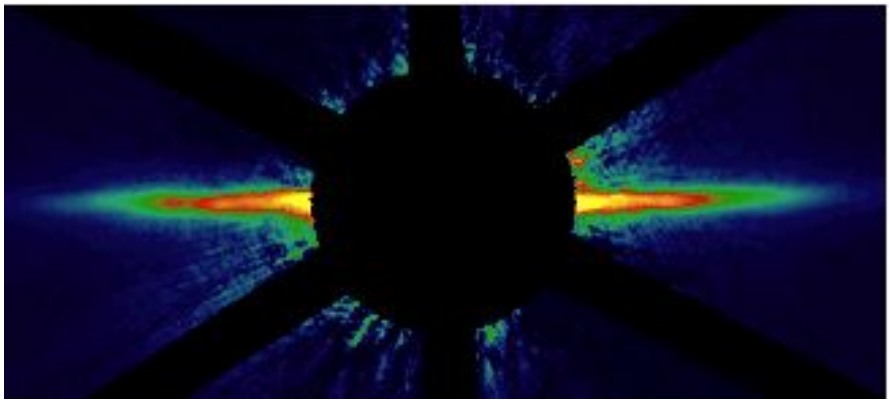

**Fig. 17** HST image of the AU Mic disk with the central regions obscured by a coronagraphic mask. AU Mic is a $12^{+8}_{-4}$ Myr old M dwarf ($\sim$0.5 $M_\odot$) only 9.9$\pm$0.1 pc from Earth. Its excess thermal emission at submillimeter wavelengths suggests a dust mass near 0.01 $M_\oplus$ (Kalas et al. 2004) while, in scattered light, it shows a nearly edge-on disk about 100 AU in diameter with evidence for structure (Liu 2004). From Liu et al. (2004).

### 8.1.3 Spectral Energy Distributions

As we mentioned above, most of the debris disks observations are spatially unresolved and are limited to the study of the SED of the star+disk system. Even assuming that the dust is distributed in a disk (and not, for example, in a spherical shell) there are degeneracies in the SED analysis and the dust distribution cannot be unambiguously determined (e.g. Moro-Moro-Martín, Wolf & Malhotra 2005a). Nevertheless, a wealth of information can be extracted from the SED. *IRAS* and *ISO* made critical discoveries on this front, but the number of known debris disks remained too small for statistical studies. This changed recently with the unprecedented sensitivity of the *Spitzer* instruments, that allowed the detection of hundreds of debris disks in large stellar surveys that searched for dust around 328 single FGK stars (Hillenbrand et al. 2008, Meyer et al. 2008, Carpenter et al. in preparation), a different sample of 293 FGK stars (Trilling et al. 2008, Beichman et al. 2006a, 2006b, Bryden et al. 2006), 160 A single stars (Su et al. 2006, Rieke et al. 2005); 69 A3–F8 binary stars (Trilling et al. 2007), and in young stellar clusters (Gorlova et al. 2007, Siegler et al. 2007). As a result, we now possess information concerning their frequencies, their dependency with stellar type and stellar environment, their temporal evolution and the composition of the dust grains (see e.g. Moro-Martín et al. 2007 for a recent review).

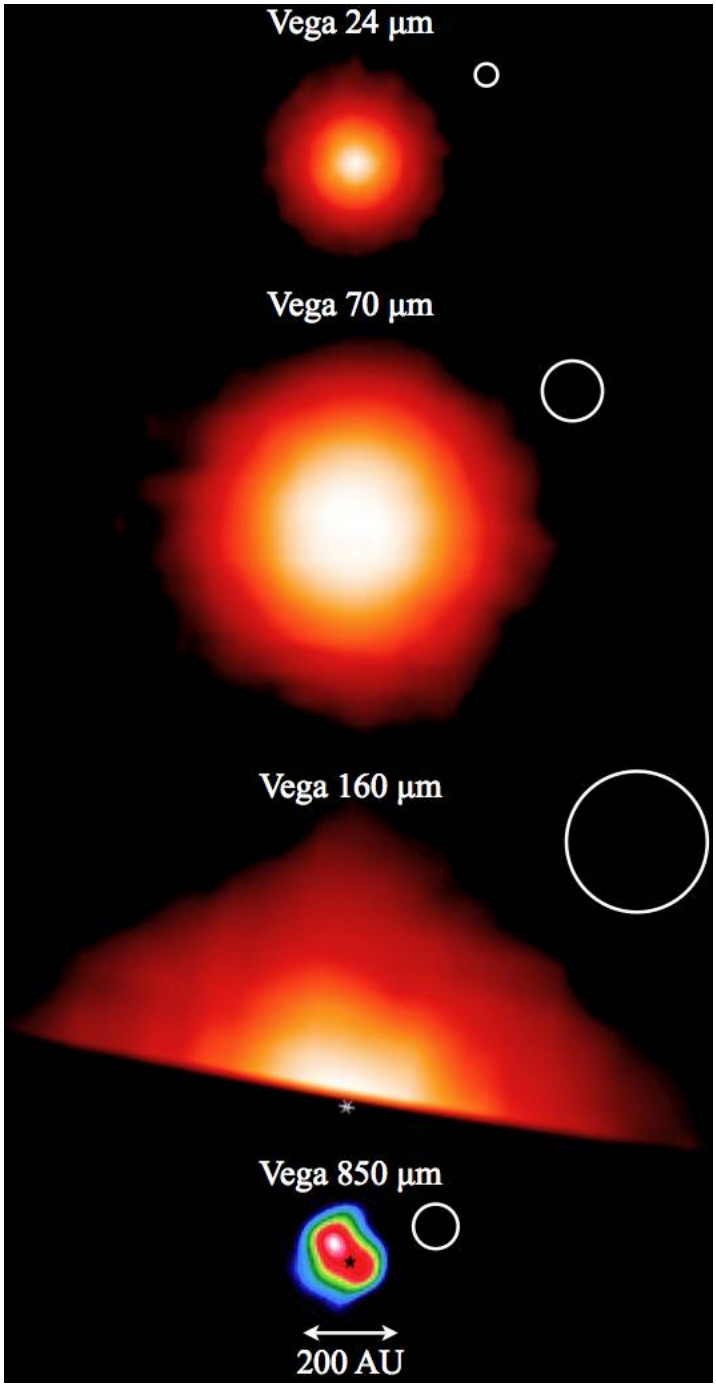


**Fig. 18** Spatially resolved images of Vega from Spitzer/MIPS at 24, 70, 160 $\mu$m (Su et al. 2005) and from JCMT/SCUBA at 850 $\mu$m (Holland et al. 1998). All images are in the same scale. The instrument beam sizes (shown in white circles) indicate that the wide radial extent of the MIPS disk images compared to the SCUBA disk image is not a consequence of the instrumental PSF but due to a different spatial location of the particles traced by the two instruments. The sub-mm emission is thought to arise from large dust particles originating from a planetesimal belt analogous to the KB, while the MIPS emission is though to correspond to smaller particles with $\beta$<0.5 (may be due to porosity), produced by collisions in the planetesimal belt traced by the sub-mm observations, and that are blown away by radiation pressure to distances much larger than the location of the parent bodies (Su et al. 2005). This scenario would explain not only the wider extent of the MIPS disk but also its uniform distribution, in contrast with the clumply and more compact sub-mm disk.

*Debris Disk Frequencies*

The *Spitzer FEPS*[2] survey of 328 FGK stars found that the frequency of 24 $\mu$m excess is 14.7% for stars younger than 300 Myr and 2% for older stars, while at 70 $\mu$m, the excess rates are 6–10% (Hilllenbrand et al. 2008 and Carpenter et al. in preparation). These disks show characteristic temperatures of 60–180 K with evidence of a population of colder grains to account for the 70 $\mu$m excesses; the implied disk inner radii are $>$ 10 AU and extend over tens of AU (see Figure 19 – Carpenter et al. in preparation). Figure 20 shows the debris disks incidence rates derived from a combined sample of 350 AFGKM stars from Trilling et al. (2008); for the 225 Sun-like (FG) stars in the sample older than 600 Myr, the frequency of the debris disks are $4.2^{+2}_{-1.1}$% at 24 $\mu$m and $16.4^{+2.8}_{-2..9}$% at 70 $\mu$m.

The above debris disks incidence rates compare to $\sim$20% of solar-type stars that harbor giant planets inside 20 AU (Marcy et al. 2005). Even though the frequencies seem similar, one should keep in mind that the sensitivity of the *Spitzer* observations is limited to fractional luminosities of $L_{dust}/L_* > 10^{-5}$, i.e. $>$100 times the expected luminosity from the KB dust in our Solar system. Assuming a gaussian distribution of debris disk luminosities and extrapolating from *Spitzer* observations (showing that the frequency of dust detection increases steeply with decreasing fractional luminosity), Bryden et al. (2006) found that the luminosity of the Solar system dust is consistent with being 10 $\times$ brighter or fainter than an average solar-type star, i.e. debris disks at the Solar system level could be common. Observations therefore indicate that planetary systems harboring dust-producing KBOs are more common than those with giant planets, which would be in agreement with the core accretion models of planet formation where the planetesimals are the building blocks of planets and the conditions required for to form planetesimals are less restricted than those to form gas giants. Indeed, there is no apparent difference between the incidence rate of debris disks around stars with and without known planetary companions (Moro-Moro-Martín et al. 2007, Bryden et al. in preparation), although planet-bearing stars tend to harbor more dusty disks (Bryden et al. in preparation), which could result from the excitation of the planetesimals' orbits by gravitational perturbations with the planet. Figure 20 shows that there is no dependency on stellar type, neither in the frequency of debris disks, nor on the dust mass and location, indicating that planetesimal formation can take place under a wide range of conditions (Trilling et al. 2008).

*Debris Disk Evolution*

The *FEPS* survey of 328 FGK stars found that at 24 $\mu$m, the frequency of excess ($>$ 10.2% over the stellar photosphere) decreases from 14.7% at ages $<$ 300 Myr to 2% for older stars; at 70 $\mu$m, there is no apparent dependency of the excess frequency with stellar age, however, the amplitude of the 70 $\mu$m excess emission seems to decline from stars 30–200 Myr in age to older stars (Hillenbrand et al. 2008

[2] http://feps.as.arizona.edu/

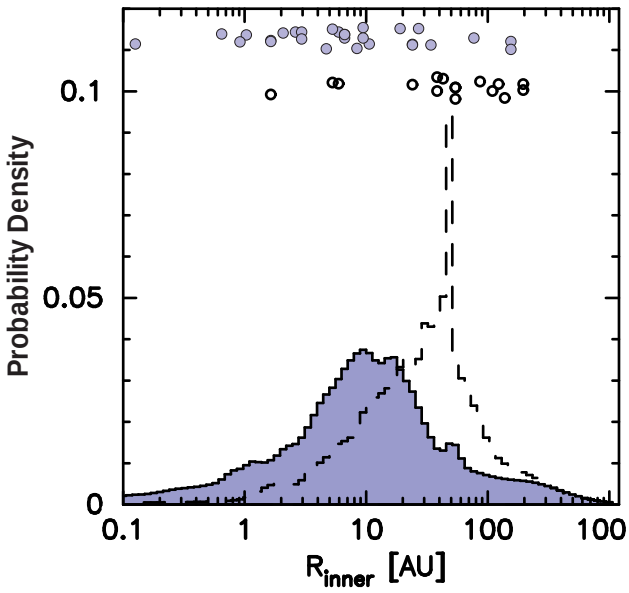


**Fig. 19** Probability distribution for disk inner radii based on the analysis of the spectra (12–35 $\mu$m) of 44 debris disks around FGK stars from the *FEPS* survey. The dashed and grey histograms correspond to sources with and without 70 $\mu$m excess, respectively (with best fit parameters are shown as open and grey circles). Typical disk inner radius are $\sim$ 40 AU and $\sim$ 10 AU for disks with and without 70 $\mu$m excess, respectively, indicating that most of the debris disks observed are KB-like. Figure adapted with permission from Carpenter et al. (in preparation).

and Carpenter et al. in preparation). Figures 21 and 22 from Trilling et al. (2008) show that for FGK type stars the debris disks incidence and fractional luminosity do not have a strong dependency with stellar age in the 1–10 Gyr time frame, in contrast with the 100–400 Myr evolution timescale of young (0.01–1 Gyr) stars seen in Figure 23. Trilling et al. (2007) argues that this data suggests that the dominant physical processes driving the evolution of the dust disks in young stars might be different from those in more mature stars, and operate on different timescales: while the former might be dominated by the production of dust during transient events like the LHB in the Solar system or by individual collisions of large planetesimals (like the one giving rise to the formation of the Moon), the later might be the result of a more steady collisional evolution of a large population of planetesimals. The debris disks evolution observed by *Spitzer* for solar-type (Figure 23 – Siegler et al. 2007) and A-type stars (Rieke et al. 2005 and Su et al. 2006) indicate that both transient and more steady state dust production processes play a role; however, their relative importance and the question of how the dust production could be maintained in the oldest disks for billions of years is still under discussion.

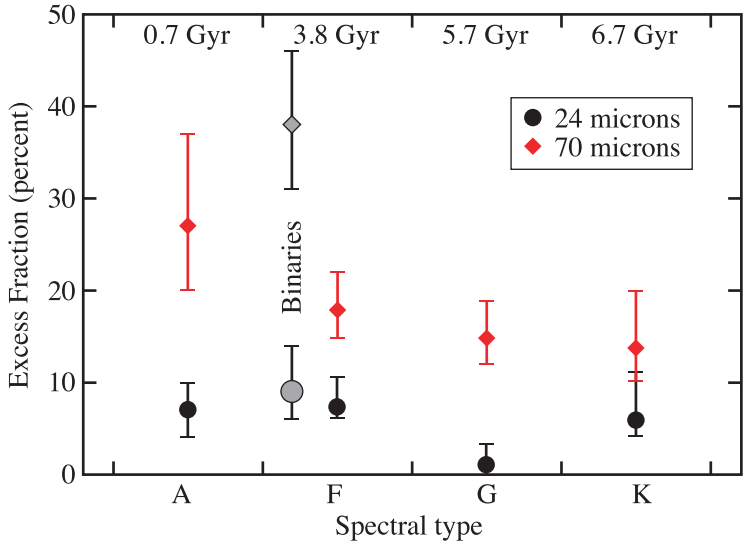


**Fig. 20** The percentage of stars showing excess dust emission, i.e. with indirect evidence of the presence of dust-producing planetesimal belts, as a function of stellar type for ages $> 600$ Myr (the mean ages within each type are shown at the top). The vertical bars correspond to binomial errors that include 68% of the probability (1 $\sigma$ for Gaussian errors). Black is for 24 $\mu$ excess emission (tracing warmer dust) and red is for 70 $\mu$ (tracing colder dust). The data are consistent with no dependence on spectral type. There seems to be a weak decrease with spectral type at 70 $\mu$ but so far this is statistically not significant and could be due to an effect of age. Further analysis indicates that percentage of stars showing excess is different in old A stars and in M stars than in FGK stars. The excess rate for old M stars is 0% with upper limits (binomial errors) of 2.9% at 24 $\mu$m and 12% at 70 $\mu$m (Gautier et al. 2007). The lack of distant disks around K stars may be an observational bias because their peak emission would be at $\lambda > 70$ $\mu$m and therefore remain undetected by *Spitzer*. The upcoming *Herschel* space telescope will provide the sensitivity to explore more distant and fainter debris disks. Figure adapted from Trilling et al. (2008) with data from Su et al. (2006), Trilling et al. (2007), Beichman et al. (2006b) and Gautier et al. (2007).

An interesting example is HD 69830, one of the outliers in Figure 24, a KOV star (0.8 $M_\odot$, 0.45 $L_\odot$) known to harbor three Neptune-like planets inside 0.63 AU. It shows a strong excess at 24 $\mu$m but no emission at 70 $\mu$m, indicating that the dust is warm and is located close to the star. The spectrum of the dust excess (Figure 24) shows strong silicate emission lines thought to arise from small grains of highly processed material similar to that of a disrupted P- or D-type asteroid plus small icy grains, likely located outside the outermost planet (Lisse et al. 2007). The observed levels of dust production are too high to be sustained for the entire age of the star, indicating that the dust production processes are transient (Wyatt et al. 2007).

Whether the disks are transient or the result of the steady erosion of planetesimals is of critical importance for the interpretation of the statistics of the incidence

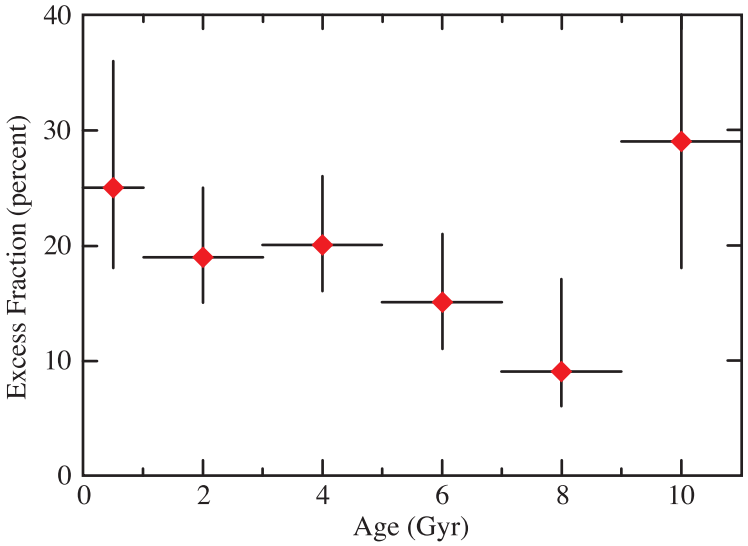


**Fig. 21** The percentage of stars showing excess dust emission, i.e. with indirect evidence of the presence of dust-producing planetesimal belts, as a function of age for the F0–K5 stars. The horizontal error bars are the age bins (not the age uncertainties). The vertical bars correspond to binomial errors that include 68% of the probability (1 $\sigma$ for Gaussian errors). The data are consistent with no dependency with age with a rate of $\sim$ 20%. The data seems to suggest an overall decrease but so far is statistically not significant, and if present may be due to an observational bias (because of the deficiency of excesses around the K stars in the oldest age bin). The number of stars in the bins are (from young to old): 24, 57, 60, 52, 33, and 7 (the high value of the oldest bin may be a small number statistical anomaly). For comparison, A-type stars evolve on timescales of 400 Myr (Su et al. 2006). Figure adapted from Trilling et al. (2008) with data from Beichman et al. (2006b).

rate of 24 $\mu$m excesses. For solar type stars, the 24 $\mu$m emission traces the 4–6 AU region. Terrestrial planet formation is expected to result in the production of large quantities of dust in this region, due to gravitational perturbations produced by large 1000 km-sized planetesimals that excite the orbits of a swarm of 1–10 km-size planetesimals, increasing their rate of mutual collisions and producing dust (Kenyon & Bromley 2005). This warm dust can therefore serve as a proxy of terrestrial planet formation. Figure 25 show the frequency of 24 $\mu$m emission for solar type (FGK) stars as a function of stellar age. This rate is $<$20% inside each age bin and decreases with age. If the dust-producing events are very long-lived, the stars that show dust excesses in one age bin will also show dust excesses at later times. In this case the frequency of warm dust (which indirectly traces the frequency of terrestrial planet formation) is $<$ 20%. However, if the dust-producing events are short-lived, shorter than the age bins, the stars showing excesses in one age bin are not the same as the stars showing excesses at other age bins, i.e. they can produce dust at different epochs, and in this case the overall frequency of warm dust is obtained from adding

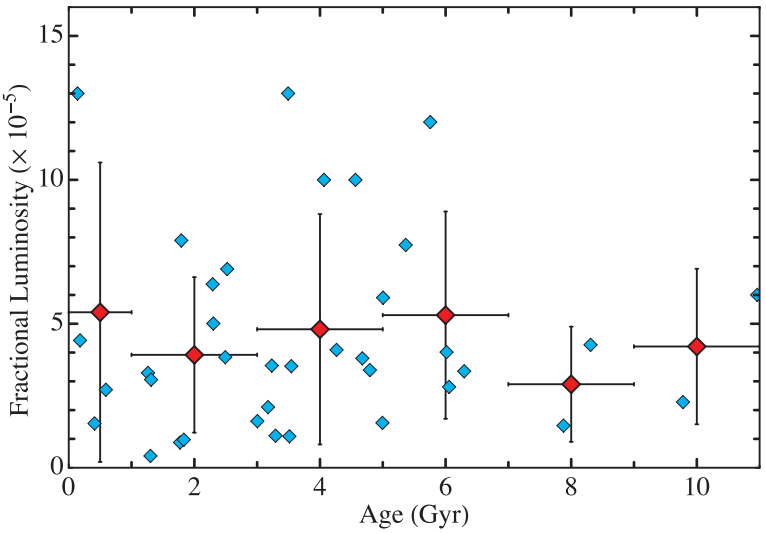


**Fig. 22** The fractional luminosity of the debris disks, $L_{dust}/L_{star}$, as a function of age for FGK stars. The open symbols show the means within each age bin; the horizontal and vertical error bars show the bin widths and 1 $\sigma$ errors, respectively. The data are consistent with no trend of $L_{dust}/L_{star}$ with age, but there seems to be a deficiency of disks with high $L_{dust}/L_{star}$ older than 6 Gyr. For comparison, the Solar system is 4.5 Gyr old and is expected to have a dust disk with $L_{dust}/L_{star} \sim 10^{-7}$–$10^{-6}$. Figure adapted from Trilling et al. (2008) with data from Beichman et al. (2006b).

all the frequencies in all age bins, which results in $> 60\%$ (assuming that each star only has one epoch of high dust production). If this is the case, the frequency of terrestrial planet formation would be high (Meyer et al. 2008). However, the interpretation of the data would change if the observed 24 $\mu$m excesses arise from the steady erosion of cold-KB-like disks (Carpenter et al., in preparation). Spatially resolved observations able to directly locate the dust would help resolve this issue.

**Next generation** facilities will offer high-sensitivity, high-resolution, multi-wavelength observations that should result in major breakthroughs in the study of debris disks. Debris disks are proxies for the presence of planetesimals around mature stars having a wide diversity of stellar types (A–K), suggesting that planetesimal formation is a robust process. The study of the warm dust can tell us about the frequency of terrestrial planet formation and the presence of asteroid-like bodies, while the study of the cold dust sheds light on the population of small bodies in KB-like regions. In addition, the study of debris

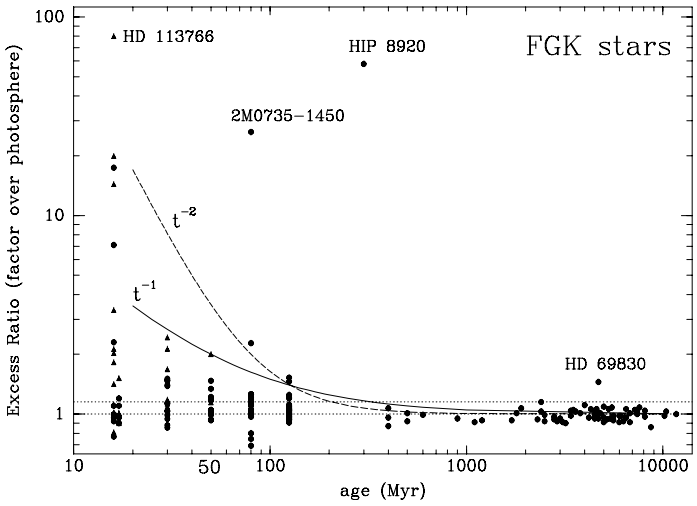


**Fig. 23** Ratio of the 24 $\mu$m Excess Emission over the expected stellar value for FGK stars as a function of stellar age (*triangles* for F0–F4 stars and *circles* for F5–K7 stars). The vertical alignments correspond to stars in clusters or associations. The data agree broadly with collisional cascade models of dust evolution (resulting in a 1/*t* decay for the dust mass) punctuated by peaks of dust production due to individual collisional events. A-type stars show a similar behavior. Figure from Siegler et al. (2007) using data from Gorlova et al. (2004), Hines et al. (2006) and Song et al. (2005).

disks around stars having a wide diversity of ages can help us learn about the evolution of planetary systems. However, the statistics so far are limited to dust disks 100–1000 $\times$ more luminous than that of our Solar system and the observations are generally spatially unresolved. High-sensitivity observations with future telescopes like *Herschel*, *JWST* and *ALMA* will be able to detect dust at the Solar system level, will help us improve our understanding of the frequency of planetesimals and, together with the result from planet searches, will show the diversity of planetary systems. Multi-wavelength observations are critical to help locate the dust in spatially unresolved disks and fundamental to interpret the debris disks statistics. High-resolution imaging observations are very important to directly locate the dust (circumventing the SED degeneracy), and to study the structure of the debris disks, perhaps serving as a planet-detection method sensitive to long-period Neptune-like planets that otherwise may be undetectable in the foreseeable future. Multi-wavelength observations also play a critical role in the interpretation of the structure because different wavelengths trace different particle sizes which have distinct dynamical characters that affect the disk morphology.

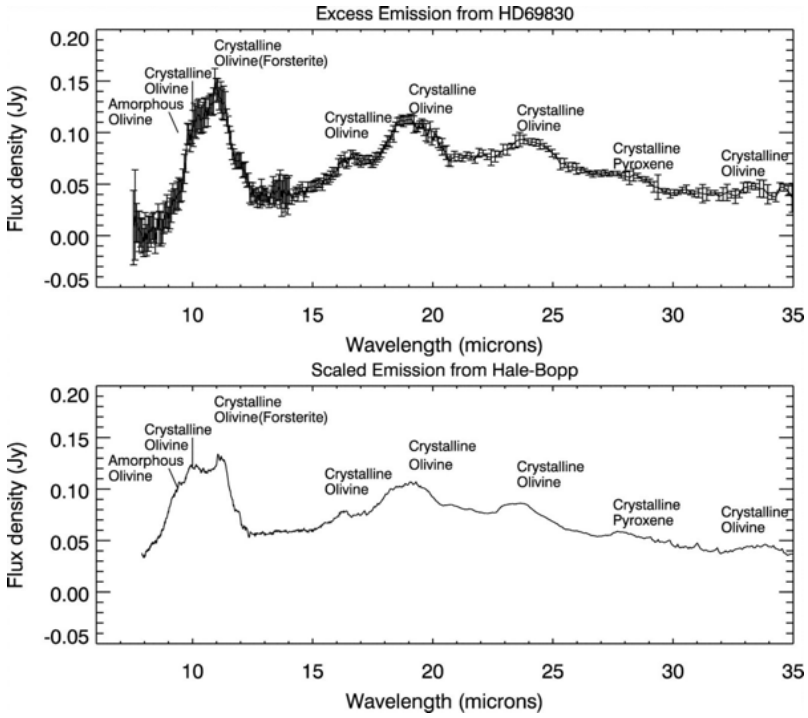


**Fig. 24** Spectrum of the dust excess emission from HD 69830 (Beichman et al. 2005 – *top*) compared to the spectrum of comet Hale-Bopp normalized to a blackbody temperature of 400 K (Crovisier et al. 1996 – *bottom*). HD 69830 is one of the outliers in Figure 23.

## *8.2 Photospheric Pollution*

Dust produced collisionally in a Kuiper belt may spiral to the central star under the action of radiation and/or plasma drag, contaminating the photosphere with metal-enriched material. Separately, gravitational interactions and dynamical instabilities in a Kuiper belt may eject large objects (comets), causing some to impact the central star. Both processes operate in our Solar system but neither produces a spectrally distinctive signature, for example a metal enrichment, on the Sun. This is simply because the photosphere of the Sun already contains a large mass of metals and the addition of dust or macroscopic bodies makes only a tiny, fractional contribution.

However, the atmospheres of some white dwarf stars offer much more favorable opportunities for the detection of a photospheric pollution signal. First, many white dwarfs are naturally depleted in metals as a result of sedimentation of heavy elements driven by their strong gravitational fields. Since their atmospheres should be very clean, quite modest masses of heavy-element pollutants can be detected. About one fifth of white dwarfs expected to have pure hydrogen or pure helium atmospheres in fact show evidence for heavier elements, most likely due to pol-

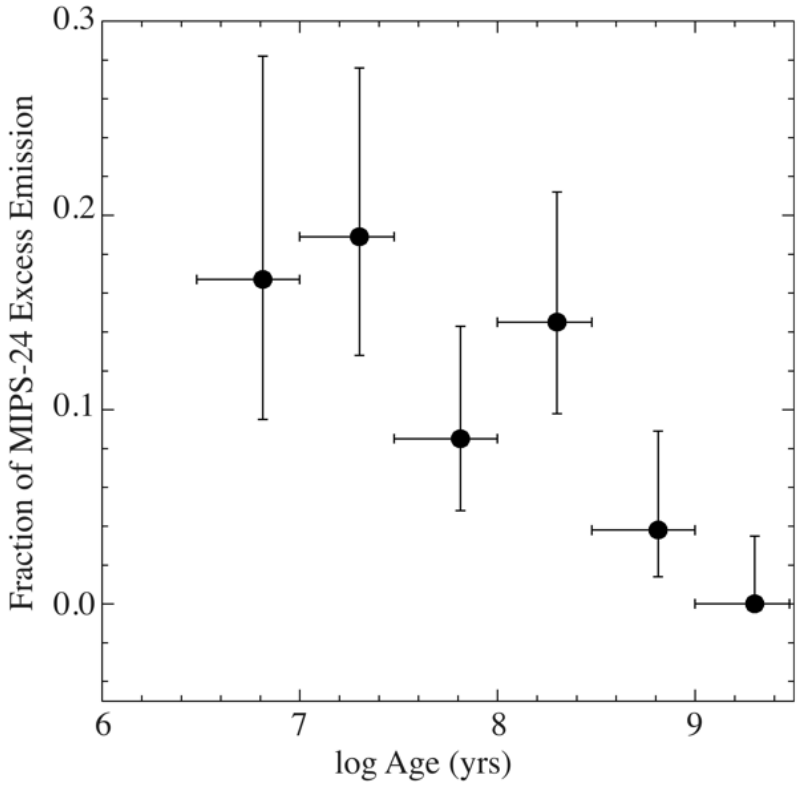


**Fig. 25** Fraction of FGK type stars with 24 $\mu$m excess emission as a function of stellar age from a sample of 328 stars. The data points correspond to average values within a given age bin: (5/30) for stars 3–10 Myr, (9/48) for 10–30 Myr, (5/59) for 30–100Myr, (9/62) for 100–300Myr, (2/53) 300–1000 Myr. The widths of the age bins are shown by the horizontal bars, while the vertical bars show Poisson errors. Figure from Meyer et al. (2008).

lution from external sources. Second, stellar evolution leading to the white dwarf stage includes the loss of stellar mass through an enhanced wind. As the central star mass decreases, the semimajor axes of orbiting bodies should increase, leading to dynamical instabilities caused by resonance sweeping and other effects (Debes and Sigurdsson 2002). Separately, white dwarf stars with Oort clouds should experience a steady flux of impacts from comets deflected inwards by stellar and galactic perturbations (Alcock et al. 1986).

An observed depletion of carbon relative to iron may suggest that the infalling material is cometary rather than of interstellar origin (Jura 2006).

## *8.3 Thermal Activation*

The blackbody temperature, in Kelvin, of an object located at distance, $R_{AU}$, from a star of luminosity, $L_\star/L_\odot$, is $T_{BB} = 278\ R_{AU}^{-1/2}(L_\star/L_\odot)^{1/4}$. In the Kuiper belt today, at $R_{AU} = 40$, the blackbody temperature is $T_{BB} = 44$ K. Water sublimation at this low temperature is negligible. However, the sublimation rate is an exponential function of temperature and, by $T_{BB} = 200$ K, water sublimates rapidly (with a mass flux $\sim 10^{-4}$ kg m$^{-2}$ s$^{-1}$, corresponding to ice recession at about 3 m yr$^{-1}$ for density 1000 kg m$^{-3}$). A 1 km scale body would sublimate away in just a few centuries. By the above relation, temperatures of 200 K are reached when $L_\star/L_\odot = 400$, for the same 40 AU distance.

Stellar evolution into the red giant phase will drive the Sun's luminosity to exceed this value after about 10 Gyr on the main-sequence, with an increase in the luminosity (by up to a factor of $\sim 10^4$), and in the loss of mass through an enhanced stellar wind (from the current value, $\sim 10^{-11}$ M$_\odot$ yr$^{-1}$, to $\sim 10^{-7}$ M$_\odot$ yr$^{-1}$, or more). When this happens, the entire Kuiper belt will light up as surface ices sublimate and dust particles, previously embedded in the KBOs, are ejected into space. Not all KBOs will be destroyed by roasting in the heat of the giant Sun: observations of comets near the Sun show that these bodies can insulate themselves from the heat by the development of refractory mantles, consisting of silicate and organic-rich debris particles that are too large to be ejected by gas drag. Still, the impact of the red giant phase should be dramatic and suggests that the sublimated Kuiper belts of other stars might be detected around red-giants. The key observational signatures would be the thermal excess itself, at temperatures appropriate to Kuiper belt-like distances, and ring-like morphology. Sensitivity at thermal wavelengths combined with high angular resolution will lend *JWST* to this type of observation, although the overwhelming signal from the star itself will present a formidable observational limitation to any imaging studies.

Water vapor has been reported around carbon stars that are not expected to show water and interpreted as produced by sublimated comets (Ford and Neufeld 2001). In IRC +10216, the mass of water is estimated as $3\times 10^{-5}$ M$_\odot$ (Melnick et al. 2001). This is about 10 M$_\oplus$, or 100 times the mass of the modern Kuiper belt but perhaps comparable to the mass of the Kuiper belt when formed. A possible explanation is that the water derives from sublimated comets in an unseen Kuiper belt, but chemical explanations for this large water mass may also be possible (Willacy 2004). On the other hand, a search for (unresolved) thermal emission from dust around 66 first-ascent red giants proved negative, with limits on the Kuiper belt masses of these stars near 0.1 M$_\oplus$, the current mass of the Kuiper belt (Jura 2004).

**Acknowledgements** DJ was supported by a grant from NASA's Origins program, PL by an NSF Planetary Astronomy grant to DJ. A.M.M. is under contract with the Jet Propulsion Laboratory (JPL) funded by NASA through the Michelson Fellowship Program. A.M.M. is also supported by the Lyman Spitzer Fellowship at Princeton University.

## References


1. Adams, F. C., & Laughlin, G. 2001: Constraints on the Birth Aggregate of the Solar System. Icarus, 150, 151
2. Alcock, C., Fristrom, C. C., & Siegelman, R. 1986: On the number of comets around other single stars. Ap. J., 302, 462
3. Anderson, J. D., Lau, E. L., Scherer, K., Rosenbaum, D. C., & Teplitz, V. L. 1998: Kuiper Belt Constraint from Pioneer 10 Icarus, 131, 167
4. Babich, D., Blake, C. H., & Steinhardt, C. L. 2007: What Can the Cosmic Microwave Background Tell Us about the Outer Solar System? Ap. J., 669, 1406
5. Backman, D. E., Dasgupta, A., & Stencel, R. E. 1995: Model of a Kuiper Belt Small Grain Population and Resulting Far-Infrared Emission. Ap. J. Lett, 450, L35
6. Backman, D. E., & Paresce, F. 1993: Main-sequence stars with circumstellar solid material - The VEGA phenomenon. Protostars and Planets III, 1253
7. Baggaley, W. J. 2000: Advanced Meteor Orbit Radar observations of interstellar meteoroids. JGR, 105, 10353
8. Bar-Nun, A., Kleinfeld, I., & Kochavi, E. 1988: Trapping of gas mixtures by amorphous water ice. Phys. Rev. B., 38, 7749
9. Barrado y Navascués, D., Stauffer, J. R., Song, I., & Caillault, J.-P. 1999: The Age of beta Pictoris. Ap. J. Lett, 520, L123
10. Beichman, C. A., et al. 2006a: IRS Spectra of Solar-Type Stars: A Search for Asteroid Belt Analogs. Ap. J., 639, 1166
11. Beichman, C. A., et al. 2006b: New Debris Disks around Nearby Main-Sequence Stars: Impact on the Direct Detection of Planets. Ap. J., 652, 1674
12. Boley, A. C., Durisen, R. H., Nordlund, Å., & Lord, J. 2007: Three-Dimensional Radiative Hydrodynamics for Disk Stability Simulations: A Proposed Testing Standard and New Results. Ap. J., 665, 1254
13. Boss, A. P. 2001: Gas Giant Protoplanet Formation: Disk Instability Models with Thermodynamics and Radiative Transfer. Ap. J., 563, 367
14. Boss, A. P. 2007: Testing Disk Instability Models for Giant Planet Formation. Ap. J. Lett., 661, L73
15. Boss, A. P., Wetherill, G. W., & Haghighipour, N. 2002: Rapid Formation of Ice Giant Planets. Icarus, 156, 291
16. Bottke, W. F., Morbidelli, A., Jedicke, R., Petit, J.-M., Levison, H. F., Michel, P., & Metcalfe, T. S. 2002: Debiased Orbital and Absolute Magnitude Distribution of the Near-Earth Objects. Icarus, 156, 399
17. Brown, M. E. 2001: The Inclination Distribution of the Kuiper Belt. Astron. J., 121, 2804
18. Brown, M. E., Trujillo, C., & Rabinowitz, D. 2004: Discovery of a Candidate Inner Oort Cloud Planetoid. Ap. J., 617, 645
19. Brownlee, D. E., Joswiak, D. J., Love, S. G., Bradley, J. P., Nier, A. O., & Schlutter, D. J. 1994: Identification and Analysis of Cometary IDPs. Lunar and Planetary Institute Conference Abstracts, 25, 185
20. Bryden, G., et al. 2006: Frequency of Debris Disks around Solar-Type Stars: First Results from a Spitzer MIPS Survey. Ap. J., 636, 1098
21. Buie, M. W., Tholen, D. J., Horne, K. 1992: Albedo maps of Pluto and Charon - Initial mutual event results. Icarus 97, 21
22. Burns, J. A., Lamy, P. L., & Soter, S. 1979: Radiation forces on small particles in the solar system. Icarus, 40, 1
23. Catullo, V., Zappala, V., Farinella, P., Paolicchi, P. 1984: Analysis of the shape distribution of asteroids. Astron. Ap. 138, 464
24. Chapman, C. R., Cohen, B. A., & Grinspoon, D. H. 2007: What are the real constraints on the existence and magnitude of the late heavy bombardment? Icarus, 189, 233
25. Crovisier, J., et al. 1996: The infrared spectrum of comet C/1995 O1 (Hale-Bopp) at 4.6 AU from the Sun.. Astron. Ap., 315, L385

26. Cruikshank, D. P., Barucci, M. A., Emery, J. P., Fernández, Y. R., Grundy, W. M., Noll, K. S., Stansberry, J. A. 2007: Physical Properties of Transneptunian Objects. Protostars and Planets V, 879
27. Davis, D. R., Farinella, P. 1997: Collisional Evolution of Edgeworth-Kuiper Belt Objects. Icarus 125, 50
28. Debes, J. H., & Sigurdsson, S. 2002: Are There Unstable Planetary Systems around White Dwarfs? Ap. J., 572, 556
29. Delsanti, A., Hainaut, O., Jourdeuil, E., Meech, K. J., Boehnhardt, H., Barrera, L. 2004: Simultaneous visible-near IR photometric study of Kuiper Belt Object surfaces with the ESO/Very Large Telescopes. Astron. Ap., 417, 1145
30. Dermott, S. F., Grogan, K., Durda, D. D., Jayaraman, S., Kehoe, T. J. J., Kortenkamp, S. J., Wyatt, M. C. 2001: Orbital evolution of interplanetary dust. Interplanetary Dust (Grum, Gustafson, Dermott, Fechtig eds.) Springer, A&A Library, pp. 569–639
31. Dermott, S. F., Jayaraman, S., Xu, Y. L., Gustafson, B. A. S., & Liou, J. C. 1994: A circumsolar ring of asteroidal dust in resonant lock with the Earth. Nature, 369, 719
32. Dermott, S. F., Kehoe, T. J. J., Durda, D. D., Grogan, K., & Nesvorný, D. 2002: Recent rubble-pile origin of asteroidal solar system dust bands and asteroidal interplanetary dust particles. Asteroids, Comets, and Meteors: ACM 2002, 500, 319
33. Duncan, M., Quinn, T., & Tremaine, S. 1988: The origin of short-period comets. Ap. J. Lett., 328, L69
34. Duncan, M. J., & Levison, H. F. 1997: A scattered comet disk and the origin of Jupiter family comets. Science, 276, 1670
35. Elliot, J. L., et al. 2005: The Deep Ecliptic Survey: Astron. J., 129, 1117
36. Farinella, P., Paolicchi, P., Zappala, V. 1981: Analysis of the spin rate distribution of asteroids. Astron. Ap. 104, 159
37. Fernández, J. A. 1980: On the existence of a comet belt beyond Neptune. MNRAS, 192, 481
38. Fernández, J. A., & Ip, W.-H. 1984: Some dynamical aspects of the accretion of Uranus and Neptune - The exchange of orbital angular momentum with planetesimals. Icarus, 58, 109
39. Fernández, Y. R., Jewitt, D. C., Sheppard, S. S. 2001. Low Albedos Among Extinct Comet Candidates. Astrophysical Journal 553, L197-L200.
40. Ford, K. E. S., & Neufeld, D. A. 2001: Water Vapor in Carbon-rich Asymptotic Giant Branch Stars from the Vaporization of Icy Orbiting Bodies. Ap. J. Lett., 557, L113
41. Francis, P. J. 2005: The Demographics of Long-Period Comets. Ap. J., 635, 1348
42. Gaidos, E. J. 1995: Paleodynamics: Solar system formation and the early environment of the sun. Icarus, 114, 258
43. Gautier, T. N., III, et al. 2007: Far-Infrared Properties of M Dwarfs. Ap. J., 667, 527
44. Gladman, B., Holman, M., Grav, T., Kavelaars, J., Nicholson, P., Aksnes, K., & Petit, J.-M. 2002: Evidence for an Extended Scattered Disk. Icarus, 157, 269
45. Gomes, R. S. 2003: The origin of the Kuiper Belt high-inclination population. Icarus 161, 404
46. Gorlova, N., et al. 2004: New Debris-Disk Candidates: 24 Micron Stellar Excesses at 100 Million years. Ap. J. Supp., 154, 448
47. Gorlova, N., Balog, Z., Rieke, G. H., Muzerolle, J., Su, K. Y. L., Ivanov, V. D., & Young, E. T. 2007: Debris Disks in NGC 2547. Ap. J., 670, 516
48. Graham, J.R., Kalas, P.G., & Matthews, B. C. 2007: The Signature of Primordial Grain Growth in the Polarized Light of the AU Microscopii Debris Disk. Ap. J., 654, 595
49. Greaves, J. S., et al. 2005: Structure in the $\epsilon$ Eridani Debris Disk. Ap. J. Lett., 619, L187
50. Grogan, K., Dermott, S. F., & Durda, D. D. 2001: The Size-Frequency Distribution of the Zodiacal Cloud: Evidence from the Solar System Dust Bands. Icarus, 152, 251
51. Grün, E., Gustafson, B., Mann, I., Baguhl, M.,
52. Grun, E., Gustafson, B., Mann, I., Baguhl, M., dust in the heliosphere. Astron. Ap., 286, 915 3125
53. Grün, Baguhl, M., Svedhem, H. & Zook, H. A. 2001: In situ measurements of cosmic dust. Interplanetary Dust (E. Grün, B. A. S. Gustafson, S. F. Dermott, H. Fechtig, eds.), Springer A&A Library, p. 293. dust in the heliosphere. Astron. Ap., 286, 915

54. Guillot, T., & Hueso, R. 2006: The composition of Jupiter: sign of a (relatively) late formation in a chemically evolved protosolar disc. MNRAS, 367, L47
55. Gurnett, D. A., Ansher, J. A., Kurth, W. S., & system by the Voyager 1 and 2 plasma wave instruments. Geoph. R. Lett., 24, 3125 24, 3125
56. Hartmann L. 2000: Accretion Processes in Star Formation, Cambridge University Press.
57. Hahn, J. M., & Malhotra, R. 1999: Orbital Evolution of Planets Embedded in a Planetesimal Disk. A. J., 117, 3041
58. Harris, A. W. 1979: Asteroid rotation rates II. A theory for the collisional evolution of rotation rates. Icarus 40, 145
59. Heap, S. R., Lindler, D. J., Lanz, T. M., Cornett, R. H., Hubeny, I., Maran, S. P., & Woodgate, B. 2000: Space Telescope Imaging Spectrograph Coronagraphic Observations of $\beta$ Pictoris. Ap. J., 539, 435
60. Higuchi, A., Kokubo, E., Kinoshita, H., & Mukai, T. 2007: Orbital Evolution of Planetesimals due to the Galactic Tide: Formation of the Comet Cloud. A. J., 134, 1693
61. Hillenbrand, L. A., et al. 2008: The Complete Census of 70-um-Bright Debris Disks within the FEPS (Formation and Evolution of Planetary Systems) Spitzer Legacy Survey of Sun-like Stars. ApJ, in press (arXiv:0801.0163).
62. Hines, D. C., et al. 2006: The Formation and Evolution of Planetary Systems (FEPS): Discovery of an Unusual Debris System Associated with HD 12039. Ap. J., 638, 1070
63. Holland, W. S., et al. 1998: Submillimetre images of dusty debris around nearby stars. Nature, 392, 788
64. Holland, W. S., et al. 2003: Submillimeter Observations of an Asymmetric Dust Disk around Fomalhaut. Ap. J., 582, 1141
65. Holland, W. S., et al. 1998: Submillimetre images of dusty debris around nearby stars. Nature, 392, 788
66. Holman, M. J., & Wisdom, J. 1993: Dynamical stability in the outer solar system and the delivery of short period comets. Astron. J., 105, 1987
67. Hsieh, H. H., & Jewitt, D. 2006: A Population of Comets in the Main Asteroid Belt. Science, 312, 561
68. Ida, S., Larwood, J., & Burkert, A. 2000: Evidence for Early Stellar Encounters in the Orbital Distribution of Edgeworth-Kuiper Belt Objects. Ap. J., 528, 351
69. Jewitt, D. C. 2002: From Kuiper Belt Object to Cometary Nucleus: The Missing Ultrared Matter. Astron. J. 123, 1039
70. Jewitt, D. 2003: Project Pan-STARRS and the Outer Solar System. Earth Moon and Planets, 92, 465
71. Jewitt, D., & Luu, J. 1993: Discovery of the candidate Kuiper belt object 1992 QB1. Nature, 362, 730
72. Jewitt, D., Luu, J. 1998: Optical-Infrared Spectral Diversity in the Kuiper Belt. Astron. J., 115, 1667
73. Jewitt, D. C., Luu, J. X. 2001: Colors and Spectra of Kuiper Belt Objects. Astron. J., 122, 2099
74. Jewitt, D., Luu, J., & Trujillo, C. 1998: Large Kuiper Belt Objects: The Mauna Kea 8K CCD Survey. Astron. J., 115, 2125
75. Jewitt, D., Peixinho, N., Hsieh, H. H. 2007: U-Band Photometry of Kuiper Belt Objects. Astron. J., 134, 2046
76. Jewitt, D. C., Sheppard, S. S. 2002: Physical Properties of Trans-Neptunian Object (20000) Varuna. Astron. J., 123, 2110
77. Jura, M. 2004: Other Kuiper Belts. Ap. J., 603, 729
78. Jura, M. 2006: Carbon Deficiency in Externally Polluted White Dwarfs: Evidence for Accretion of Asteroids. Ap. J., 653, 613
79. Kalas, P., Graham, J. R., & Clampin, M. 2005: A planetary system as the origin of structure in Fomalhaut's dust belt. Nature, 435, 1067
80. Kalas, P., Graham, J. R., & Clampin, M. 2005: A planetary system as the origin of structure in Fomalhaut's dust belt.

81. Lee, T., Papanastassiou, D. A., & Wasserburg, G. J. 1977: Aluminum-26 in the early solar system - Fossil or fuel. Ap. J. Lett., 211, L107
82. Kalas, P., Liu, M. C., & Matthews, B. C. 2004: Discovery of a Large Dust Disk Around the Nearby Star AU Microscopii. Science, 303, 1990
83. Kenyon, S. J., & Bromley, B. C. 2005: Prospects for Detection of Catastrophic Collisions in Debris Disks. Astron. J., 130, 269
84. Kuchner, M. J., & Holman, M. J. 2003: The Geometry of Resonant Signatures in Debris Disks with Planets. Ap. J., 588, 1110
85. Lacerda, P., Jewitt, D. C. 2007: Densities of Solar System Objects from Their Rotational Light Curves. Astron. J., 133, 1393
86. Lacerda, P., Jewitt, D., Peixinho, N. 2008: High Precision Photometry of Extreme KBO 2003 EL61. In press in Astron. J.
87. Lacerda, P., Luu, J. 2003: On the detectability of lightcurves of Kuiper belt objects. Icarus 161, 174
88. Lacerda, P., Luu, J. 2006: Analysis of the Rotational Properties of Kuiper Belt Objects. Astron. J., 131, 2314
89. Leinert, C., Roser, S., & Buitrago, J. 1983: How to maintain the spatial distribution of interplanetary dust. Astron. Ap., 118, 345
90. Leinert, C., & Grün, E. 1990: Interplanetary Dust. Physics of the Inner Heliosphere I, 207
91. Levison, H. F., & Duncan, M. J. 1994:The long-term dynamical behavior of short-period comets. Icarus, 108, 18
92. Levison, H. F., Dones, L., & Duncan, M. J. 2001: The Origin of Halley-Type Comets: Probing the Inner Oort Cloud. A. J., 121, 2253
93. Levison, H. F., Terrell, D., Wiegert, P. A., Dones, L., & Duncan, M. J. 2006:On the origin of the unusual orbit of Comet 2P/Encke. Icarus, 182, 161
94. Liou, J.-C., & Zook, H. A. 1997: Evolution of Interplanetary Dust Particles in Mean Motion Resonances with Planets. Icarus, 128, 354
95. Liu, M. C. 2004: Substructure in the Circumstellar Disk Around the Young Star AU Microscopii. Science, 305, 1442
96. Luu, J., Jewitt, D. 1996: Color Diversity Among the Centaurs and Kuiper Belt Objects. Astron. J., 112, 2310
97. Luu, J., Lacerda, P. 2003: The Shape Distribution Of Kuiper Belt Objects. Earth Moon and Planets 92, 221
98. Luu, J., Marsden, B. G., Jewitt, D., Trujillo, C. A., Hergenrother, C. W., Chen, J., & Offutt, W. B. 1997: A New Dynamical Class in the Trans-Neptunian Solar System. Nature, 387, 573
99. Marcy, G., Butler, R. P., Fischer, D., Vogt, S., Wright, J. T., Tinney, C. G., & Jones, H. R. A. 2005: Observed Properties of Exoplanets: Masses, Orbits, and Metallicities. Progress of Theoretical Physics Supplement, 158, 24
100. Malhotra, R. 1995: The Origin of Pluto's Orbit: Implications for the Solar System Beyond Neptune. Astron. J., 110, 420
101. Melnick, G. J., Neufeld, D. A., Ford, K. E. S., Hollenbach, D. J., & Ashby, M. L. N. 2001: Discovery of water vapour around IRC+10216 as evidence for comets orbiting another star. Nature, 412, 160
102. Meyer, M. R., et al. 2008: Evolution of Mid-Infrared Excess around Sun-like Stars: Constraints on Models of Terrestrial Planet Formation. Ap. J. Lett., 673, L181
103. Moro-Martín, A., & Malhotra, R. 2002: A Study of the Dynamics of Dust from the Kuiper Belt: Spatial Distribution and Spectral Energy Distribution. Astron. J., 124, 2305
104. Moro-Martín, A., & Malhotra, R. 2003: Dynamical Models of Kuiper Belt Dust in the Inner and Outer Solar System. Astron. J., 125, 2255
105. Moro-Martín, A., Wolf, S., & Malhotra, R. 2005a: Signatures of Planets in Spatially Unresolved Debris Disks. Ap. J., 621, 1079
106. Moro-Martín, A., & Malhotra, R. 2005b: Dust Outflows and Inner Gaps Generated by Massive Planets in Debris Disks. Ap. J., 633, 1150
107. Moro-Martín, A., et al. 2007: Are Debris Disks and Massive Planets Correlated?. Ap. J., 658, 1312

108. Moro-Martin, A., Wyatt, M. C., Malhotra, R., & Trilling, D. E. 2008: Extra-Solar Kuiper Belt Dust Disks. The Solar System Beyond Neptune (A. Barucci, H. Boehnhardt, D. Cruikshank, A. Morbidelli, eds.) University of Arizona Press, Tucson. arXiv:astro-ph/0703383
109. Morbidelli, A., & Levison, H. F. 2004: Scenarios for the Origin of the Orbits of the Trans-Neptunian Objects 2000 CR105 and 2003 VB12 (Sedna). Astron. J, 128, 2564
110. Mostefaoui, S., Lugmair, G. W., Hoppe, P., & El Goresy, A. 2004: Evidence for live $^{60}$Fe in meteorites. New Astronomy Review, 48, 155
111. Oort, J. H. 1950: The structure of the cloud of comets surrounding the Solar System and a hypothesis concerning its origin. Bull. Astron. Inst. Neth., 11, 91
112. Ouellette, N., Desch, S. J., & Hester, J. J. 2007: Interaction of Supernova Ejecta with Nearby Protoplanetary Disks. Ap. J., 662, 1268
113. Owen, T., Mahaffy, P., Niemann, H. B., Atreya, S., Donahue, T., Bar-Nun, A., & de Pater, I. 1999: A low-temperature origin for the planetesimals that formed Jupiter. Nature, 402, 269
114. Paresce, F. 1991: On the evolutionary status of Beta Pictoris. Astron. Ap., 247, L25
115. Peixinho, N., Doressoundiram, A., Delsanti, A., Boehnhardt, H., Barucci, M. A., Belskaya, I. 2003: Reopening the TNOs color controversy: Centaurs bimodality and TNOs unimodality. Astronomy and Astrophysics 410, L29.
116. Reach, W. T., Morris, P., Boulanger, F., & Okumura, K. 2003: The mid-infrared spectrum of the zodiacal and exozodiacal light. Icarus, 164, 384
117. Rice, W. K. M., & Armitage, P. J. 2003: On the Formation Timescale and Core Masses of Gas Giant Planets. Ap. J. Lett., 598, L55
118. Rieke, G. H., et al. 2005: Decay of Planetary Debris Disks. Ap. J., 620, 1010
119. Schneider, G., Silverstone, M. D., & Hines, D. C. 2005: Discovery of a Nearly Edge-on Disk around HD 32297. Ap. J. Lett., 629, L117
120. Siegler, N., Muzerolle, J., Young, E. T., Rieke, G. H., Mamajek, E. E., Trilling, D. E., Gorlova, N., & Su, K. Y. L. 2007: Spitzer 24 $\mu$m Observations of Open Cluster IC 2391 and Debris Disk Evolution of FGK Stars. Ap. J., 654, 580
121. Sheppard, S. S., Jewitt, D. C. 2002: Time-resolved Photometry of Kuiper Belt Objects: Rotations, Shapes, and Phase Functions. Astron. J., 124, 1757
122. Sheppard, S. S., Jewitt, D. 2004: Extreme Kuiper Belt Object 2001 QG298 and the Fraction of Contact Binaries. Astron. J., 127, 3023
123. Sheppard, S. S., Lacerda, P., & Ortiz, J.-L. 2008: Photometric Lightcurves of Transneptunian Objects and Centaurs: Rotations, Shapes, and Densities. In "The Solar System Beyond Neptune" (Eds. Barucci, A. et al.), Univ. Az. Press, Tucson, pp. 129
124. Sheppard, S. S., & Trujillo, C. A. 2006: A Thick Cloud of Neptune Trojans and Their Colors. Science, 313, 511
125. Song, I., Zuckerman, B., Weinberger, A. J., & Becklin, E. E. 2005: Extreme collisions between planetesimals as the origin of warm dust around a Sun-like star. Nature, 436, 363
126. Stapelfeldt, K. R., et al. 2004: First Look at the Fomalhaut Debris Disk with the Spitzer Space Telescope. Ap. J. Supp., 154, 458
127. Stern, S. A. 1996: Signatures of collisions in the Kuiper Disk.. Astron. Ap., 310, 999
128. Strom, R. G., Malhotra, R., Ito, T., Yoshida, F., & Kring, D. A. 2005: The Origin of Planetary Impactors in the Inner Solar System. Science, 309, 1847
129. Su, K. Y. L., et al. 2005: The Vega Debris Disk: A Surprise from Spitzer. Ap. J., 628, 487
130. Su, K. Y. L., et al. 2006: Debris Disk Evolution around A Stars. Ap. J., 653, 675
131. Sykes, M. V., & Greenberg, R. 1986: The formation and origin of the IRAS zodiacal dust bands as a consequence of single collisions between asteroids. Icarus, 65, 51
132. Tegler, S. C., Romanishin, W. 2000: Extremely red Kuiper-belt objects in near-circular orbits beyond 40 AU. Nature 407, 979
133. Thébault, P., Doressoundiram, A. 2003: Colors and collision rates within the Kuiper belt: problems with the collisional resurfacing scenario. Icarus 162, 27
134. Trafton, L. M. 1989: Pluto's atmosphere near perihelion. Geophysical Research Letters 16, 1213
135. Trilling, D. E., et al. 2007: Debris disks in main-sequence binary systems.. Ap. J., 658, 1289

136. Trilling, D. E., et al. 2008: Debris Disks around Sun-like Stars. Ap. J., 674, 1086
137. Trujillo, C. A., Jewitt, D. C., & Luu, J. X. 2001: Properties of the Trans-Neptunian Belt. Astron. J. 122, 457
138. Willacy, K. 2004: A Chemical Route to the Formation of Water in the Circumstellar Envelopes around Carbon-rich Asymptotic Giant Branch Stars: Fischer-Tropsch Catalysis. Ap. J. Lett., 600, L87
139. Wyatt, M. C., Dermott, S. F., Telesco, C. M., Fisher, R. S., Grogan, K., Holmes, E. K., & Piña, R. K. 1999: How Observations of Circumstellar Disk Asymmetries Can Reveal Hidden Planets: Pericenter Glow and Its Application to the HR 4796 Disk. Ap. J., 527, 918
140. Wyatt, M. C., Smith, R., Greaves, J. S., Beichman, C. A., Bryden, G., & Lisse, C. M. 2007: Transience of Hot Dust around Sun-like Stars. Ap. J., 658, 569
141. Yamamoto, S., & Mukai, T. 1998: Dust production by impacts of interstellar dust on Edgeworth-Kuiper Belt objects. Astron. Ap., 329, 785
142. Young, E. F., Galdamez, K., Buie, M. W., Binzel, R. P., Tholen, D. J. 1999: Mapping the Variegated Surface of Pluto. Astron. J., 117, 1063
143. Zook, H. A., & Berg, O. E. 1975: A source for hyperbolic cosmic dust particles. Planetary and Space Sciences, 23, 183